Detecting Marine Species in Echograms via Traditional, Hybrid, and Deep Learning Frameworks

Tunai Porto Marques *[1], Alireza Rezvanifar *[1], Melissa Cote [1], Alexandra Branzan Albu [1],
Kaan Ersahin [2], Todd Mudge [2], Stephane Gauthier [3]
*: equal contribution

[1] University of Victoria, BC, Canada
[2] ASL Environmental Sciences, Victoria, Canada
[3] Institute of Ocean Sciences, Fisheries and Oceans Canada, Sidney, BC, Canada

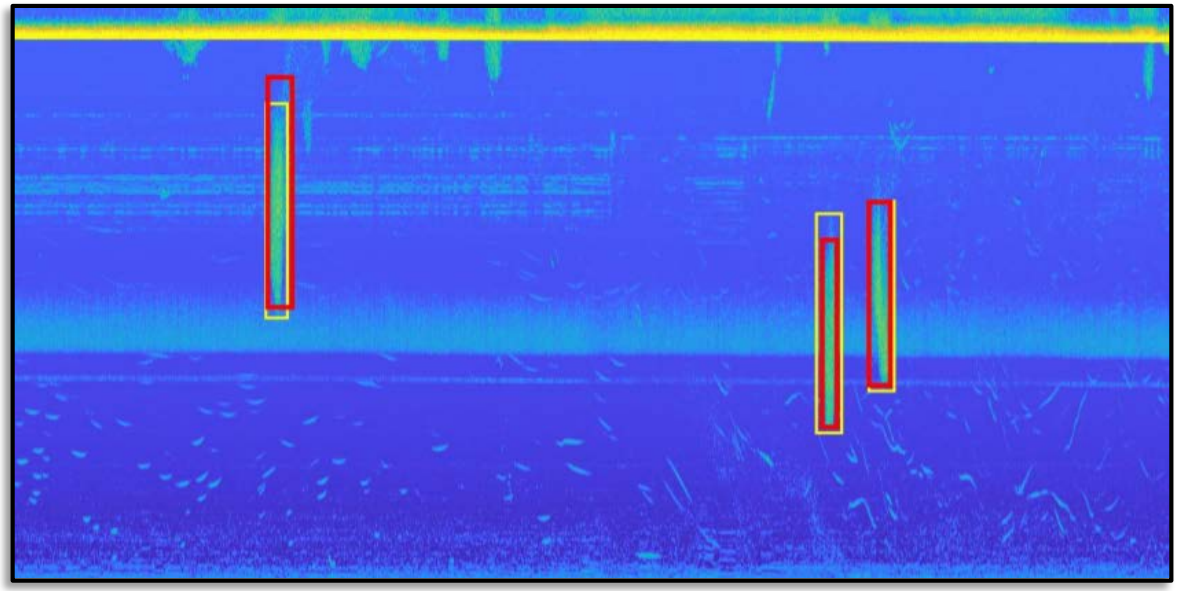

25th International Conference on Pattern Recognition. Milan, Italy, January 10-15 2021

Marine biologists and acousticians: acoustic monitoring

- Non-invasive
- Thorough

Marine biologists and acousticians: acoustic monitoring

- Non-invasive
- Thorough

Echosounders: ASL Environmental Science's AZFP [1]

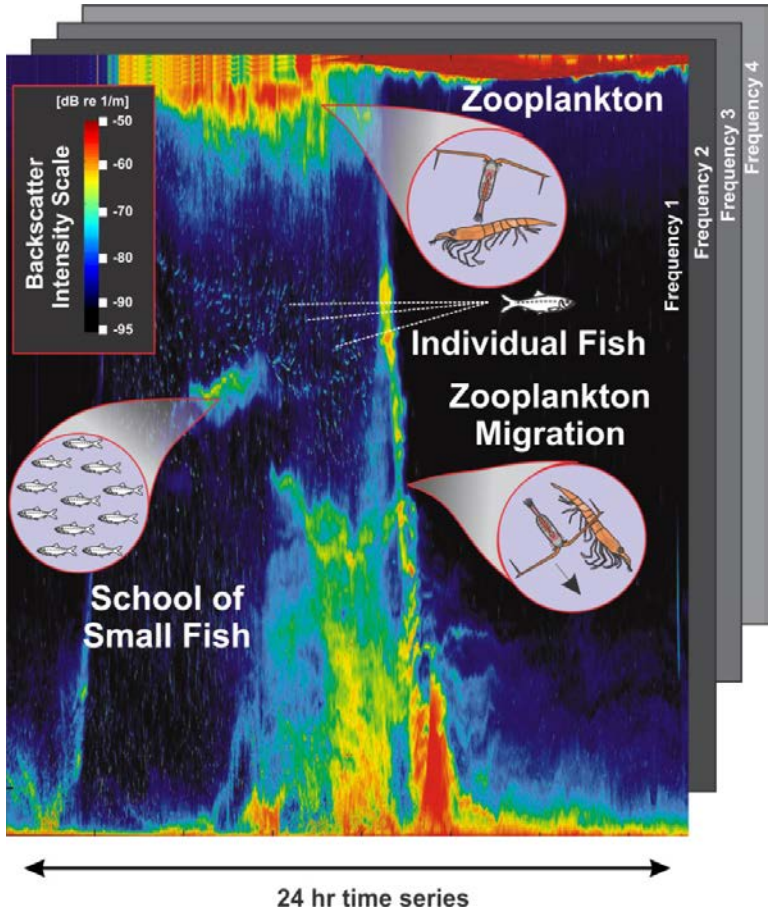

Illustration of an AZFP-generated echogram [1]

Marine biologists and acousticians: acoustic monitoring

- Non-invasive
- Thorough

Echosounders: ASL Environmental Science's AZFP [1]

Manual or semi-automatic methods:

- Time-consuming
- Prone to inter-expert disagreements

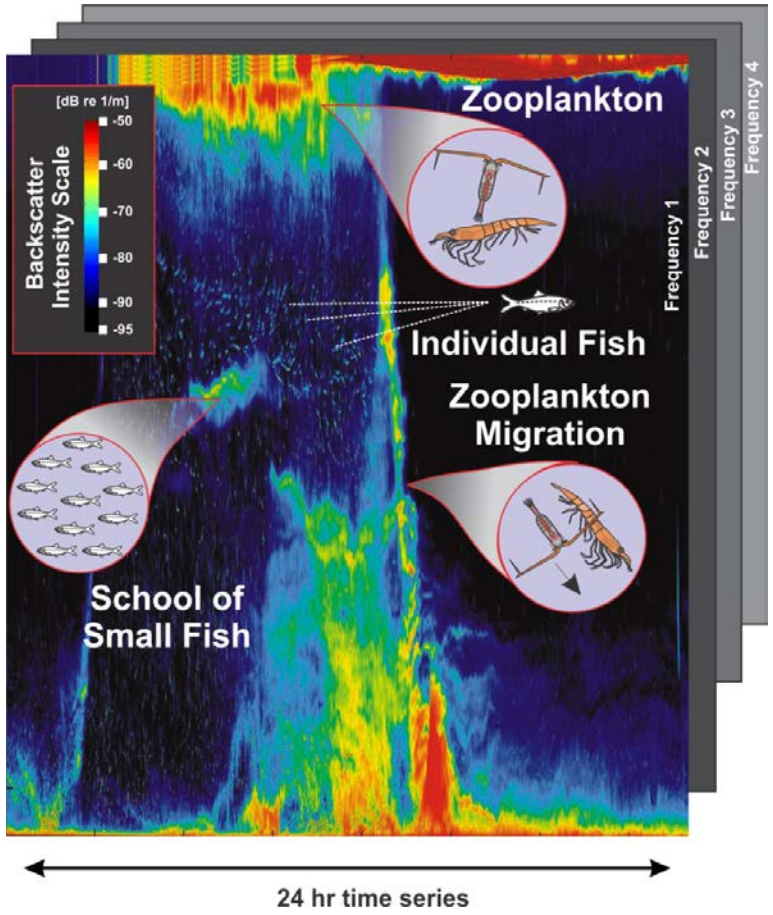

Illustration of an AZFP-generated echogram [1].

Marine biologists and acousticians: acoustic monitoring

- Non-invasive
- Thorough

Echosounders: ASL Environmental Science's AZFP [1]

Manual or semi-automatic methods:

- Time-consuming
- Prone to inter-expert disagreements

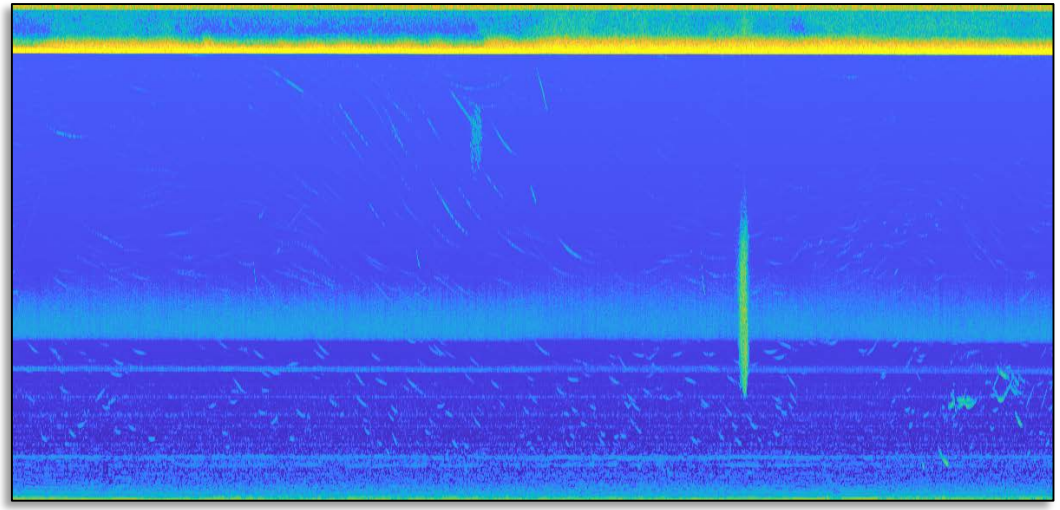

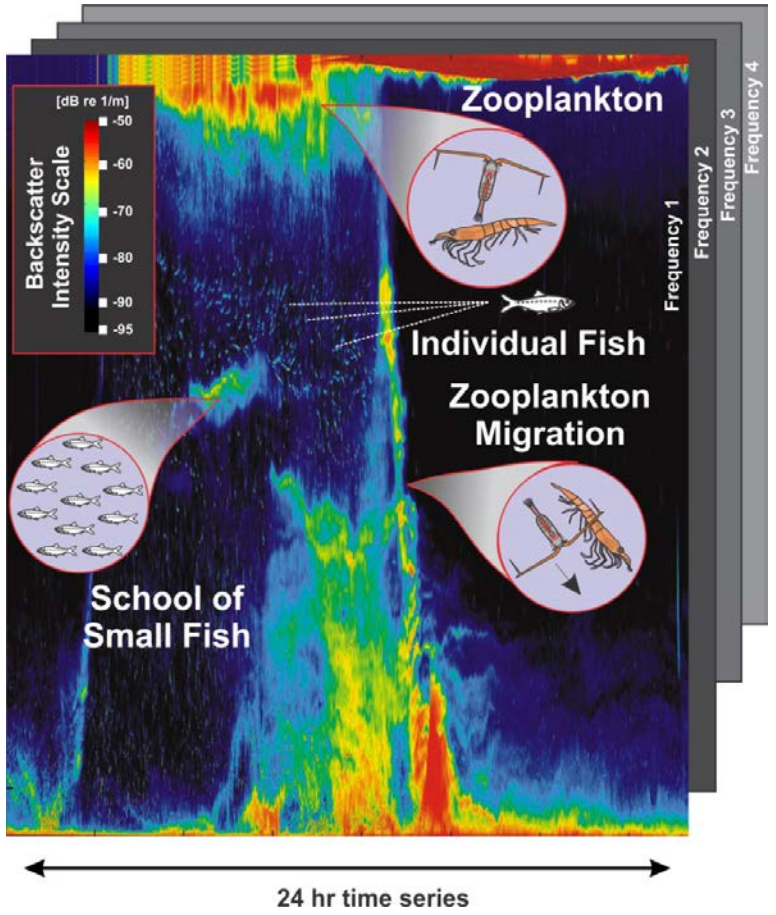

Illustration of an AZFP-generated echogram [1].

Marine biologists and acousticians: acoustic monitoring

- Non-invasive
- Thorough

Echosounders: ASL Environmental Science's AZFP [1]

Manual or semi-automatic methods:

- Time-consuming
- Prone to inter-expert disagreements

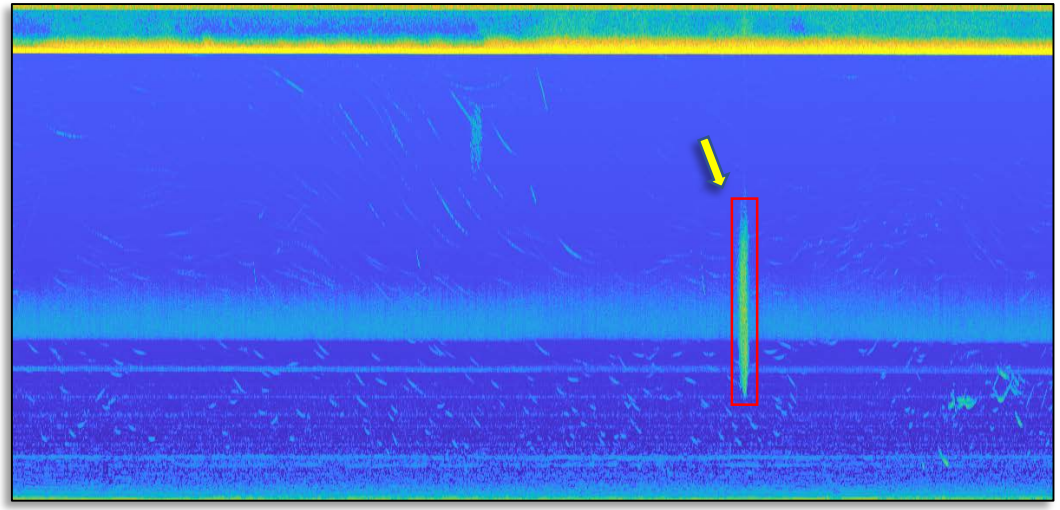

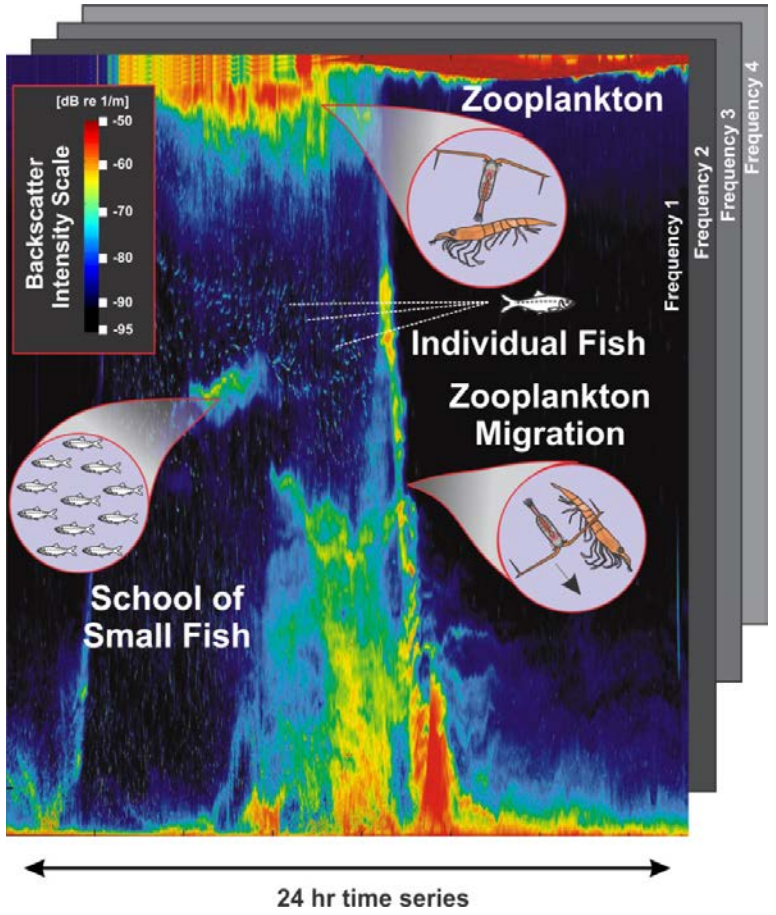

Illustration of an AZFP-generated echogram [1].

Perform a comparison between machine learning-based approaches for the automatic detection of marine species in echograms.

Marine biologists and acousticians: acoustic monitoring

- Non-invasive
- Thorough

Echosounders: ASL Environmental Science's AZFP [1]

Manual or semi-automatic methods:

- Time-consuming
- Prone to inter-expert disagreements

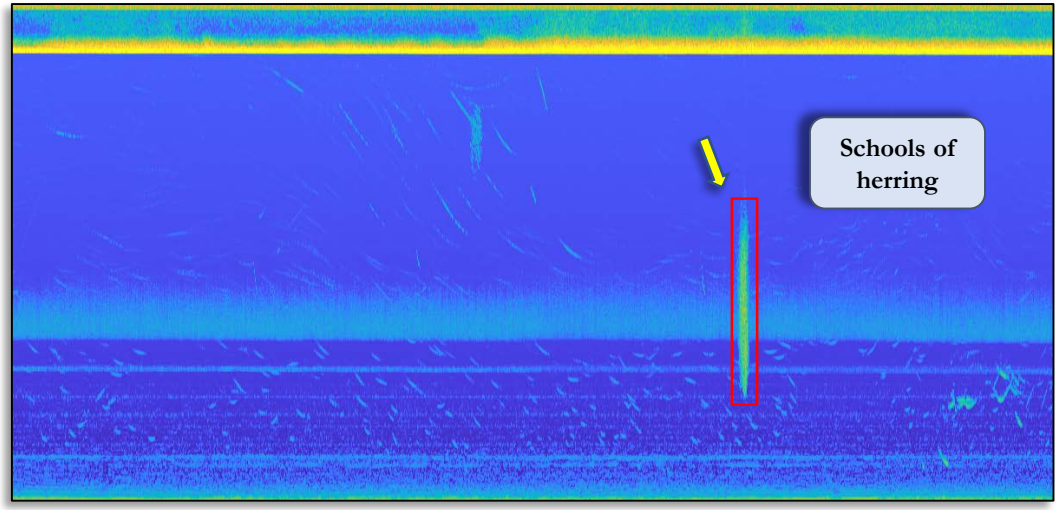

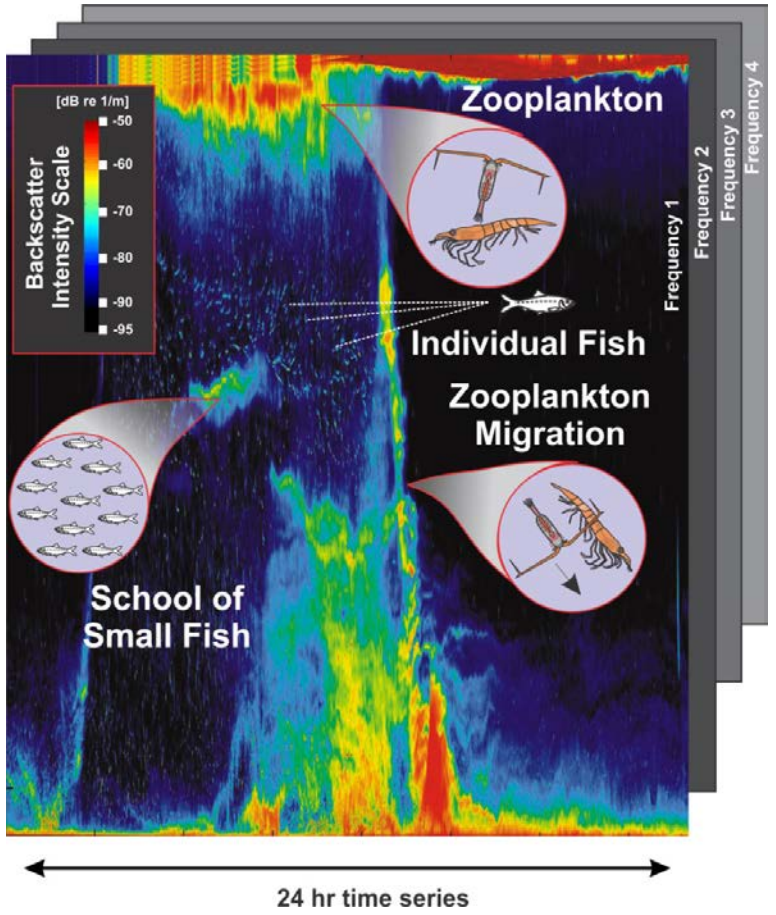

Illustration of an AZFP-generated echogram [1].

Perform a comparison between machine learning-based approaches for the automatic detection of ***marine species*** *in echograms.*

Multi-frequency, heterogeneous morphology

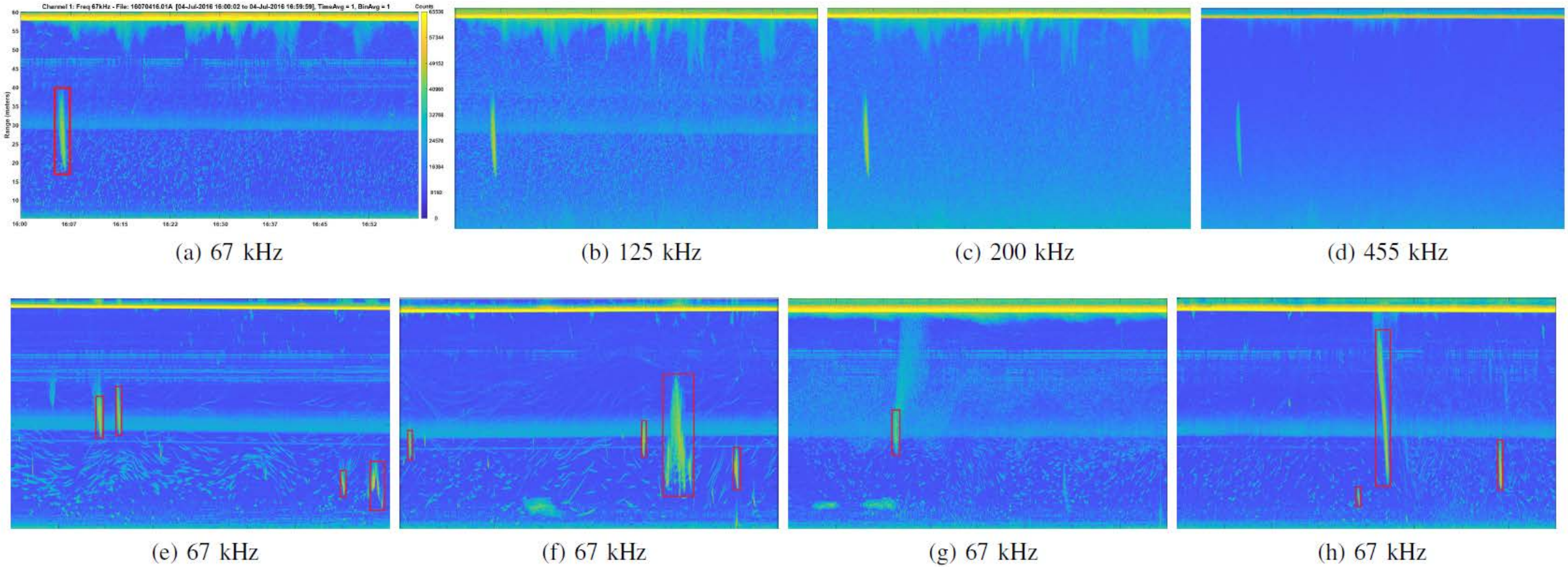

(a) 67 kHz (b) 125 kHz (c) 200 kHz (d) 455 kHz

(e) 67 kHz (f) 67 kHz (g) 67 kHz (h) 67 kHz

Sample 1-hour echograms measured with a fixed-position echosounder (see Sec. III-A). First row: (a) 67 kHz echogram with range (*y*-) and time (*x*-) axes, and acoustic echo intensity; (b)-(d) the same echogram at other frequencies. Second row: four echograms (only 67 kHz is shown) containing various schools identified by red bounding boxes.

Machine learning-based approaches

Approach	Localization	Classification
1) Hand-crafted	Custom ROI extractor	ML image classifier
2) Hybrid	Custom ROI extractor	DL image classifier
3) End-to-end	DL object detector	DL object detector

ROI = region of interest, ML = machine learning, DL = deep learning

Machine learning-based approaches

Hand-crafted

- Most common in the related literature (see Sec. I-B from the manuscript)
- Novel Region of Interest (ROI) extractor
  - Herring-specific assumptions
- Support Vector Machine (SVM)
  - Four hand-crafted features

Approach	Localization	Classification
1) Hand-crafted	Custom ROI extractor	ML image classifier
2) Hybrid	Custom ROI extractor	DL image classifier
3) End-to-end	DL object detector	DL object detector

ROI = region of interest, ML = machine learning, DL = deep learning

Machine learning-based approaches

Hand-crafted

- Most common in the related literature (see Sec. I-B from the manuscript)
- Novel Region of Interest (ROI) extractor
  - Herring-specific assumptions
- Support Vector Machine (SVM)
  - Four hand-crafted features

Hybrid

- Novel Region of Interest (ROI) extractor
  - Herring-specific assumptions
- Custom deep learning-based image classifiers (ResNet [22], DenseNet[23], Inception [24])

Approach	Localization	Classification
1) Hand-crafted	Custom ROI extractor	ML image classifier
2) Hybrid	Custom ROI extractor	DL image classifier
3) End-to-end	DL object detector	DL object detector

ROI = region of interest, ML = machine learning, DL = deep learning

Machine learning-based approaches

Hand-crafted

- Most common in the related literature (see Sec. I-B from the manuscript)
- Novel Region of Interest (ROI) extractor
  - Herring-specific assumptions
- Support Vector Machine (SVM)
  - Four hand-crafted features

Hybrid

- Novel Region of Interest (ROI) extractor
  - Herring-specific assumptions
- Custom deep learning-based image classifiers (ResNet [22], DenseNet[23], Inception [24])

End-to-end

- Custom-trained end-to-end object detectors (Faster R-CNN [25], YOLOv2 [26])
- Novel tiling approach

Approach	Localization	Classification
1) Hand-crafted	Custom ROI extractor	ML image classifier
2) Hybrid	Custom ROI extractor	DL image classifier
3) End-to-end	DL object detector	DL object detector

ROI = region of interest, ML = machine learning, DL = deep learning

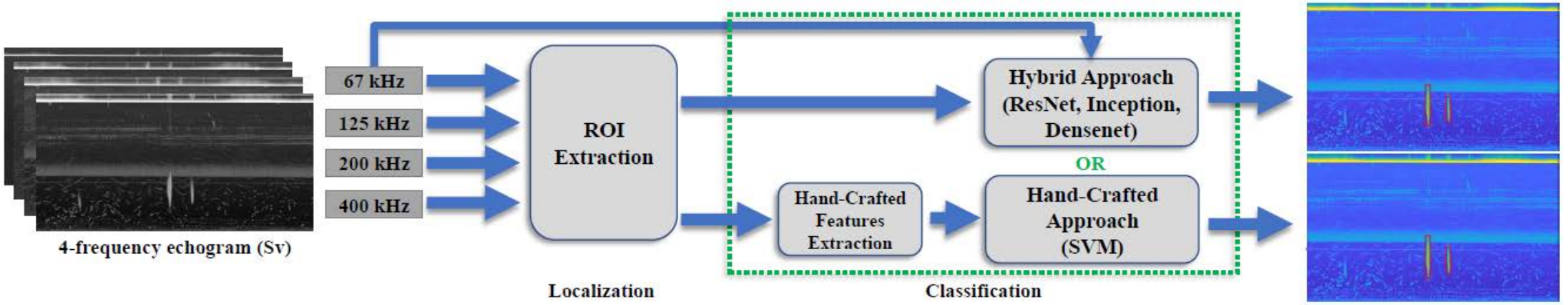

(a)

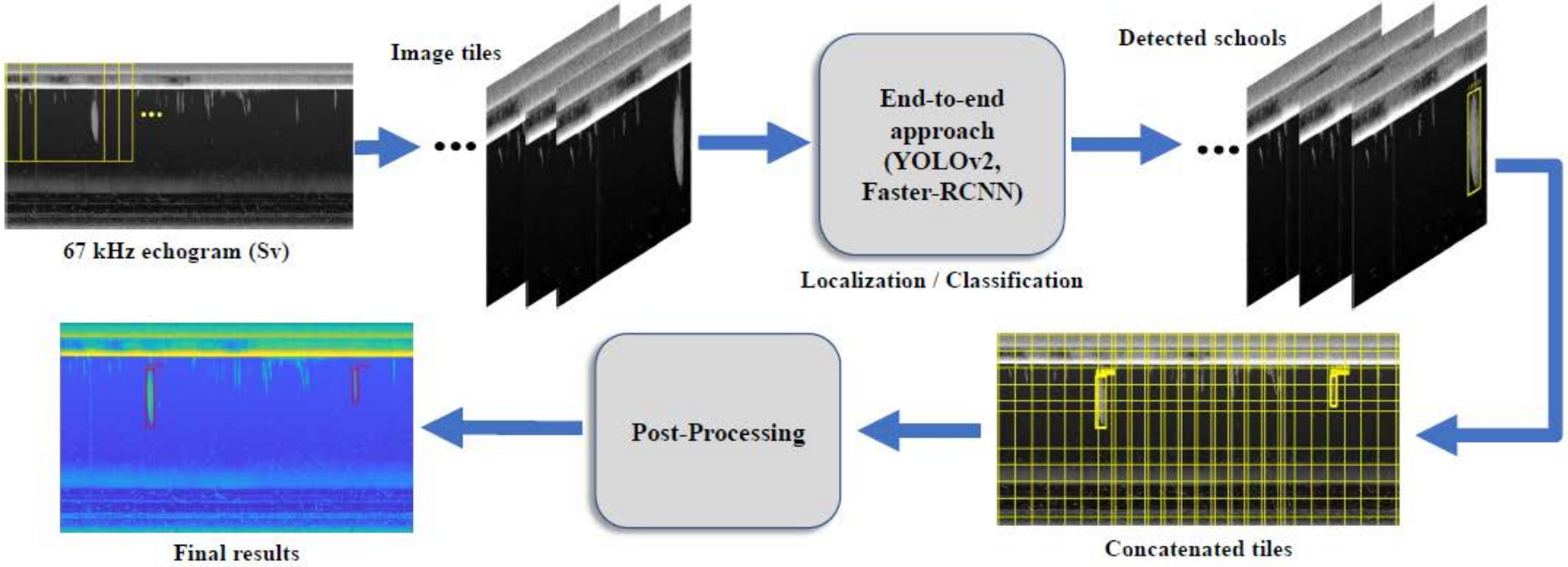

(b)

General block diagram of hand-crafted and hybrid approaches (a) and end-to-end approach (b). Red bounding boxes highlight the identified targets in the final results, shown on colour-coded echograms for better visualization.

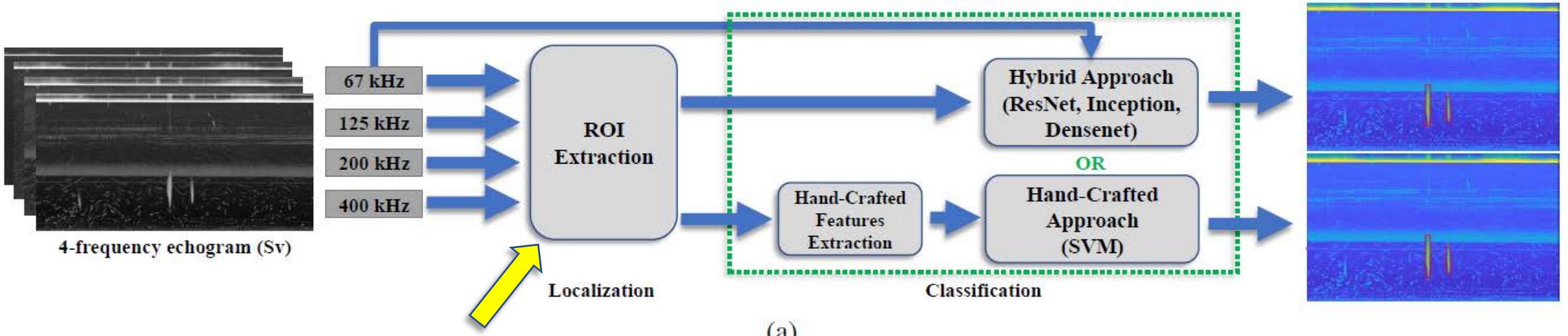

(a)

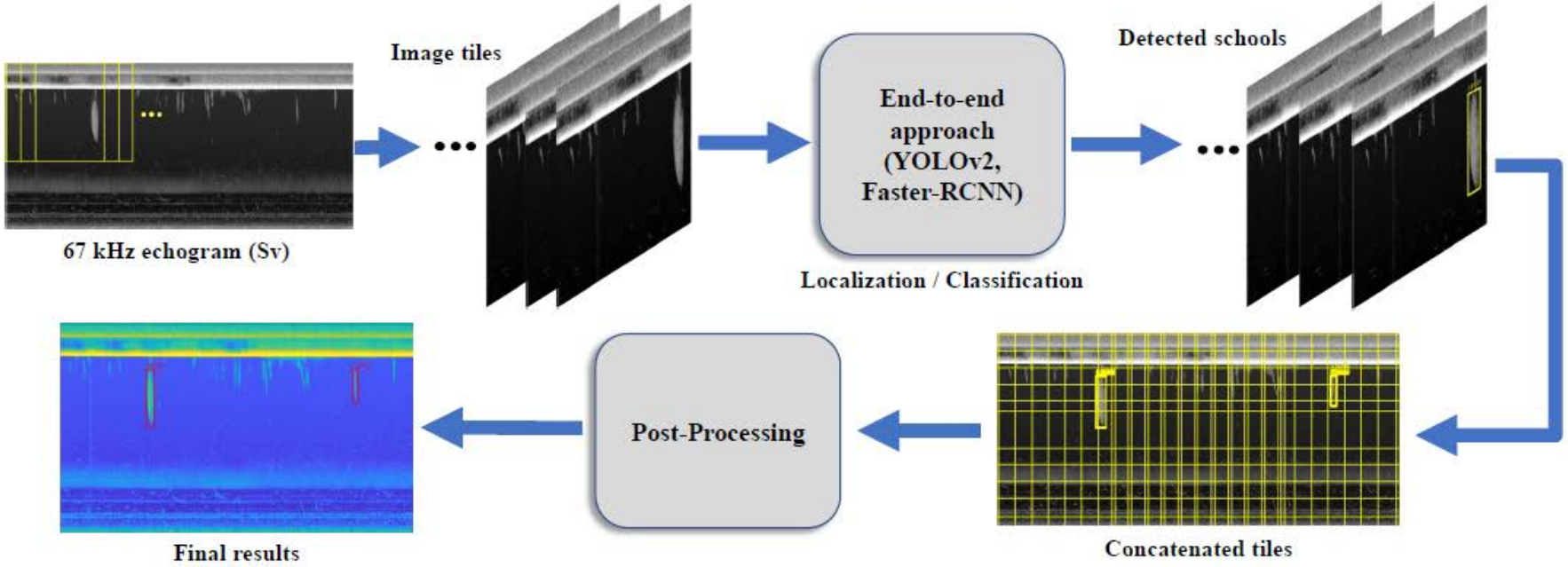

(b)

General block diagram of hand-crafted and hybrid approaches (a) and end-to-end approach (b). Red bounding boxes highlight the identified targets in the final results, shown on colour-coded echograms for better visualization.

Region of Interest (ROI) extractor

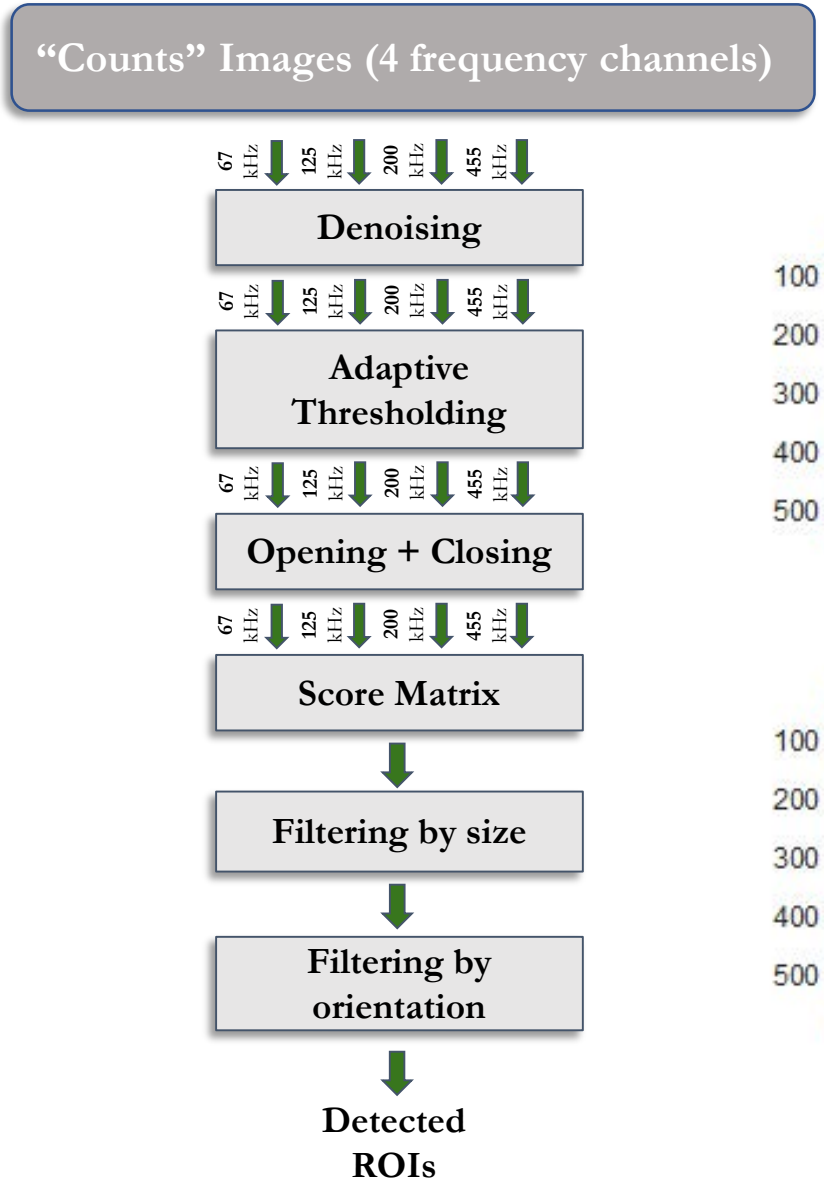

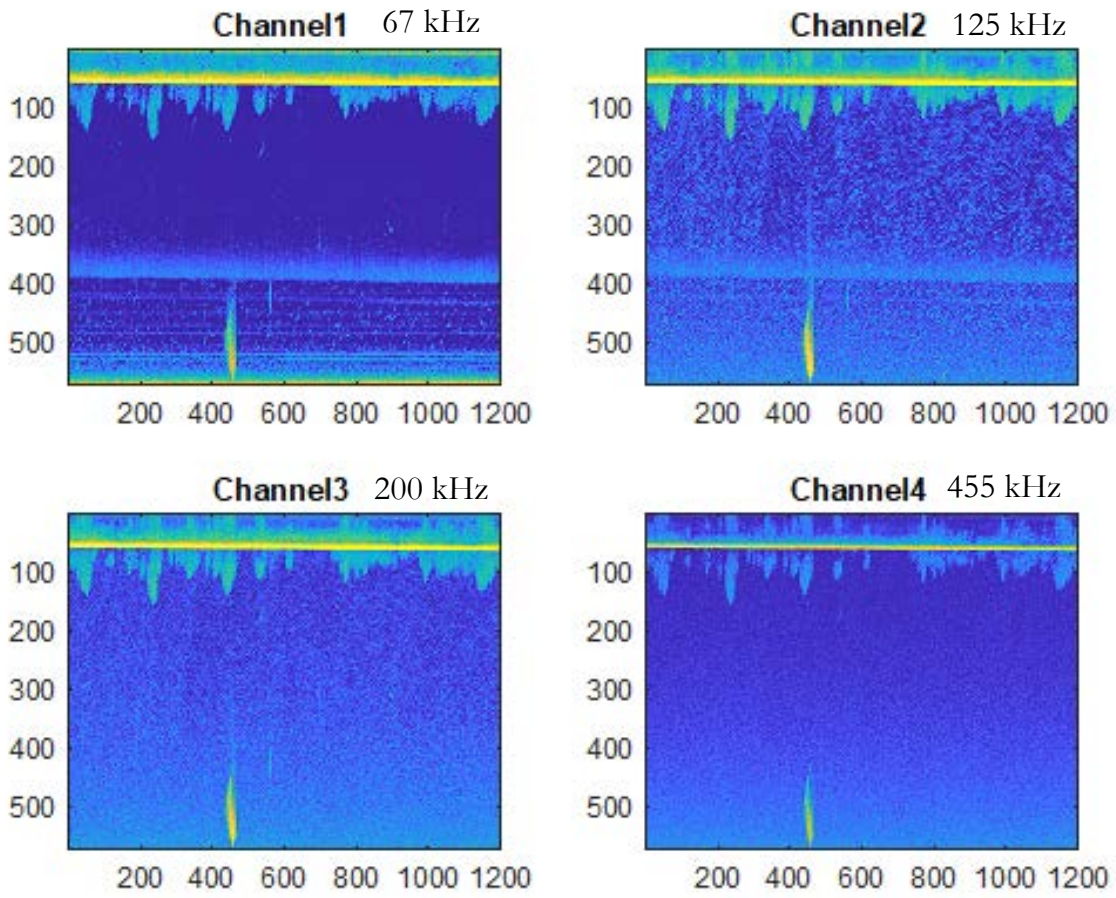

Echograms from the same site captured using four different frequencies.

Region of Interest (ROI) extractor

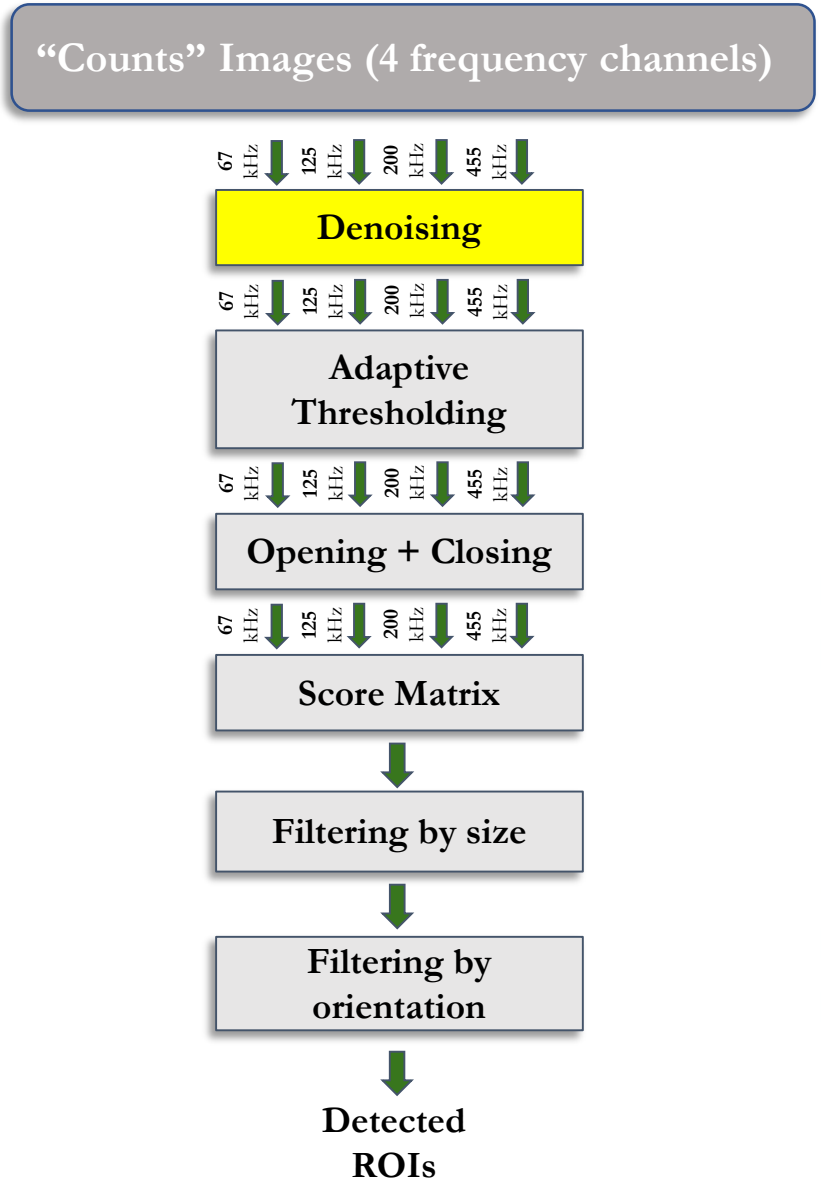

- Median filter on the x-axis (time direction)
- Short signals (individual fish)

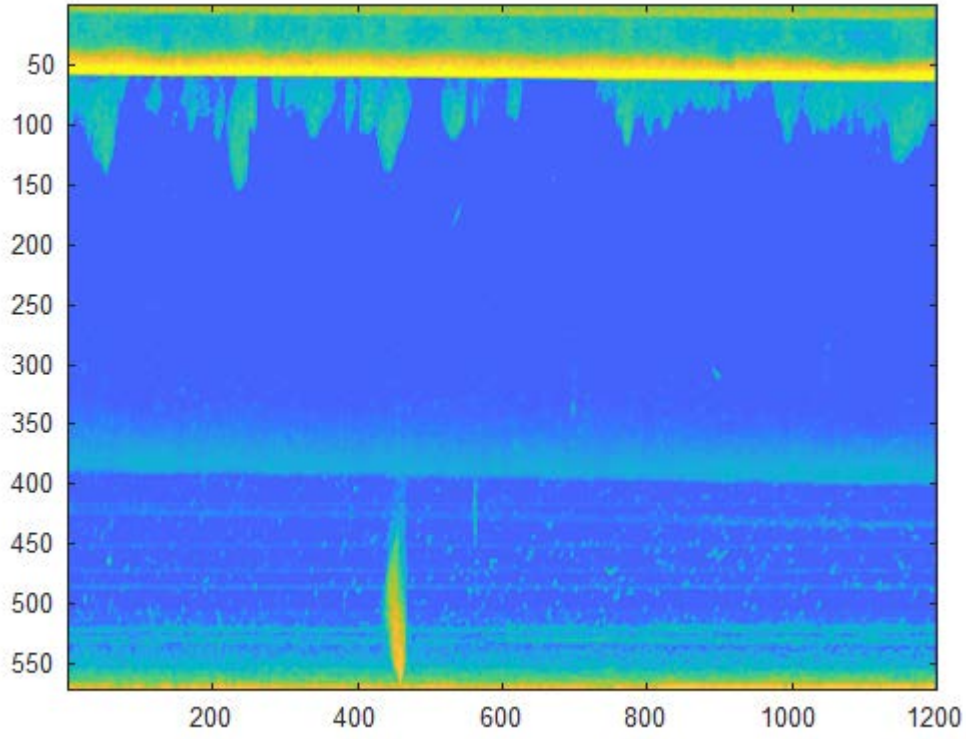

Result of the median filtering (67 kHz shown).

Region of Interest (ROI) extractor

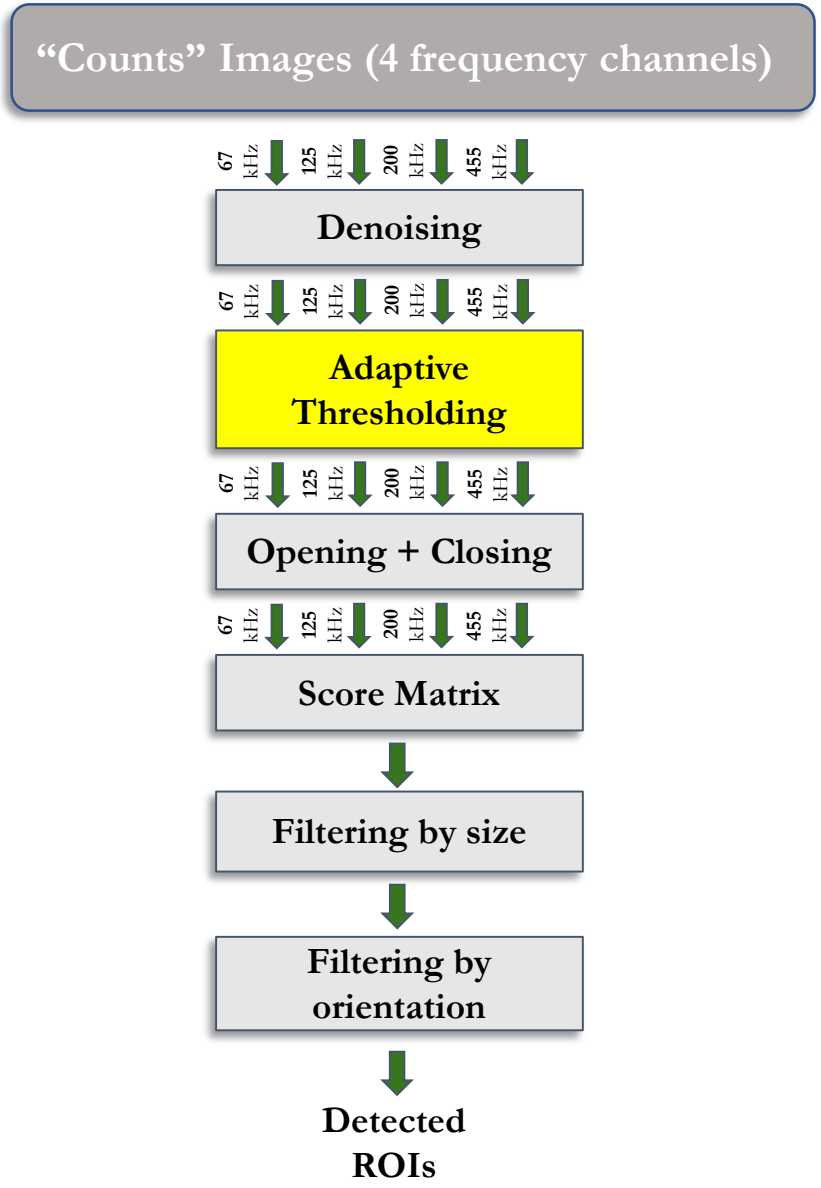

- Region-specific thresholding

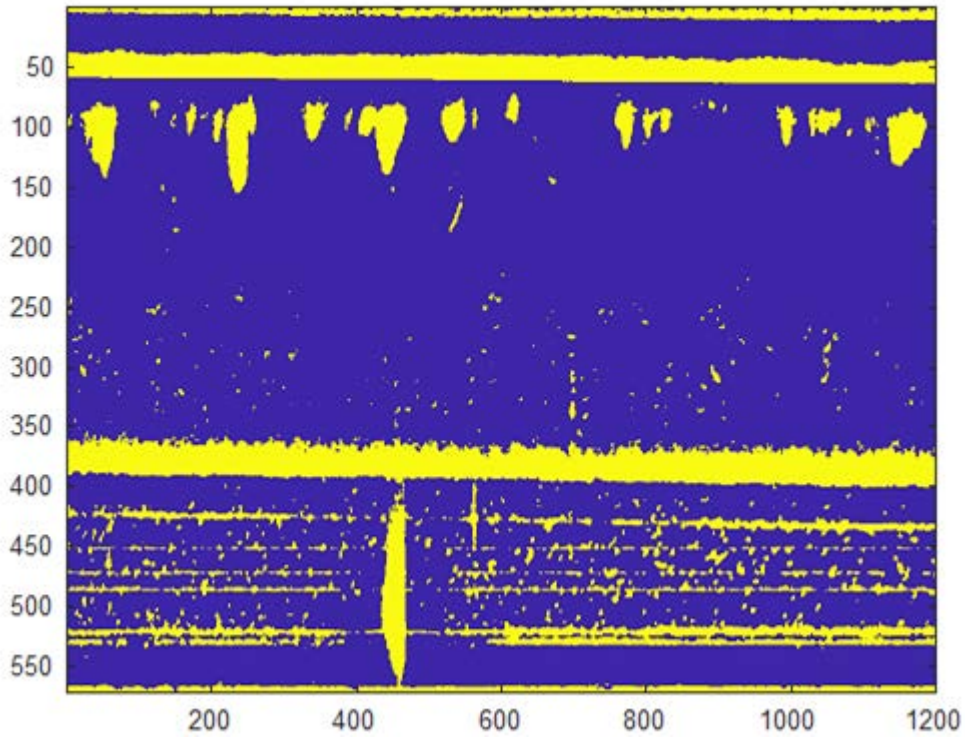

Result of the adaptive thresholding (67 kHz shown).

Region of Interest (ROI) extractor

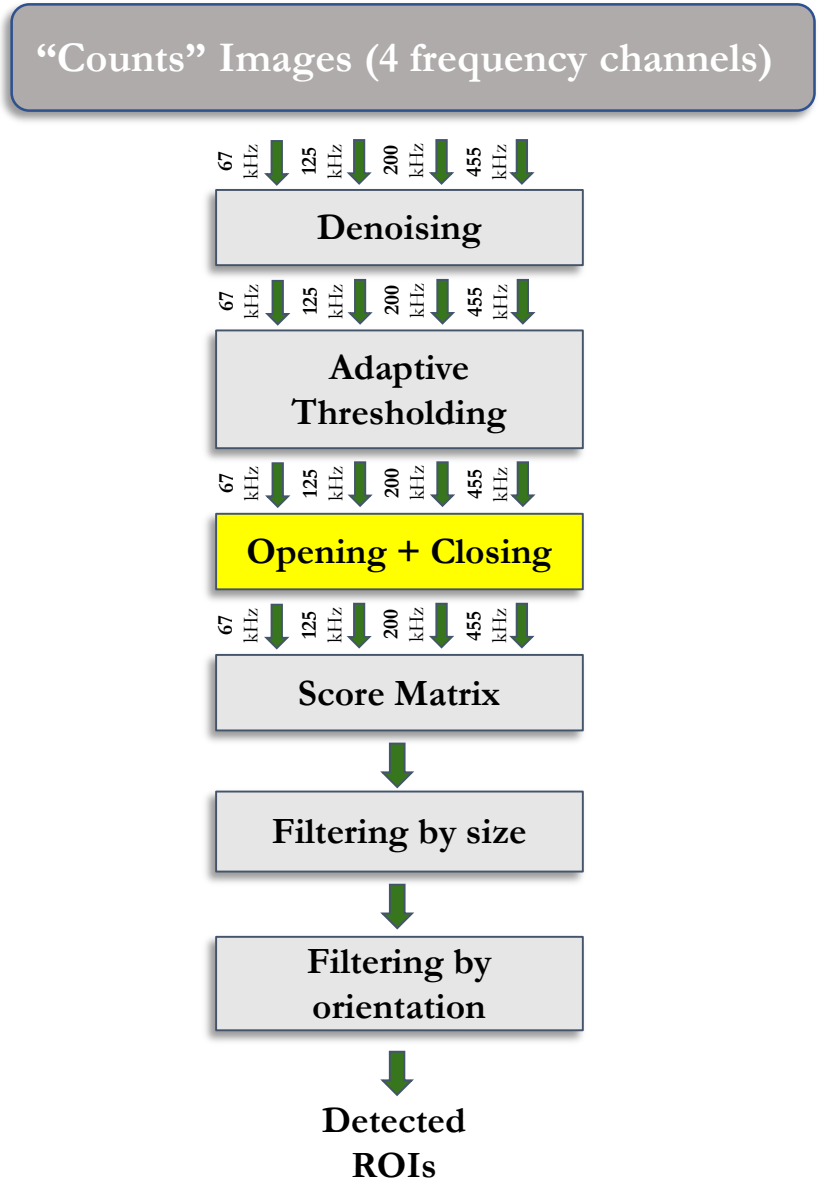

- Removes small sets of connected components

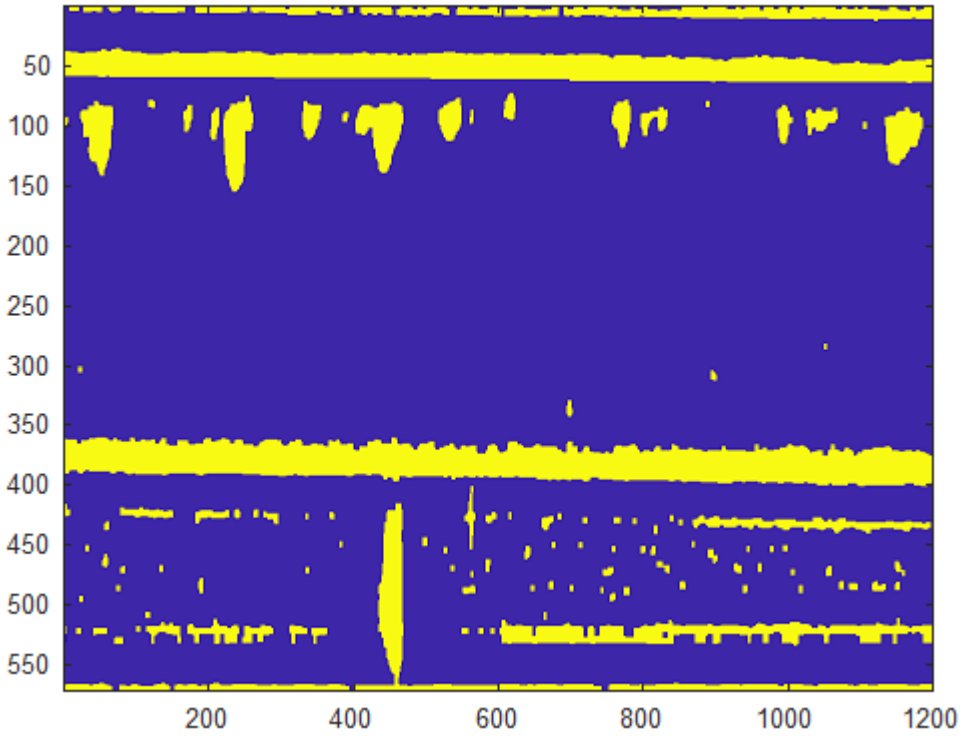

Result of the morphological operations (67 kHz shown).

Region of Interest (ROI) extractor

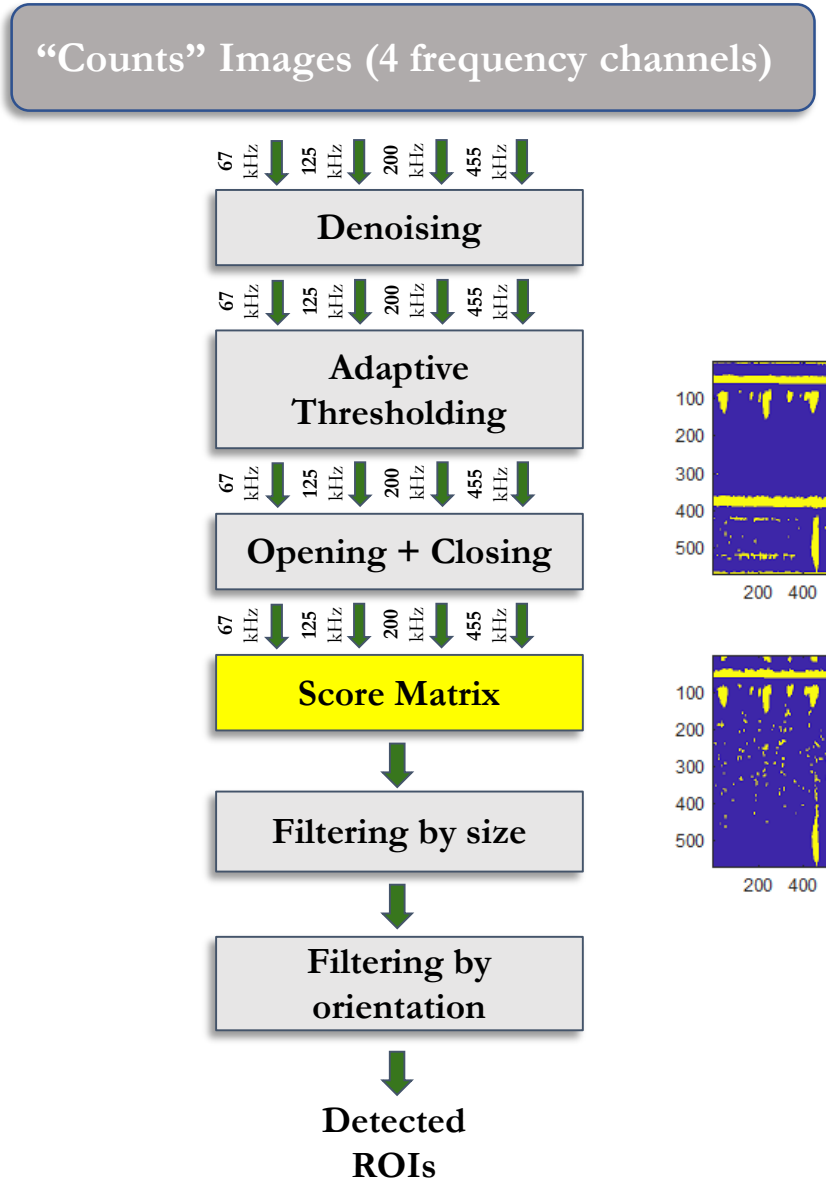

- Sum the values on all four frequencies (binary)
- Max value for a given position: 4

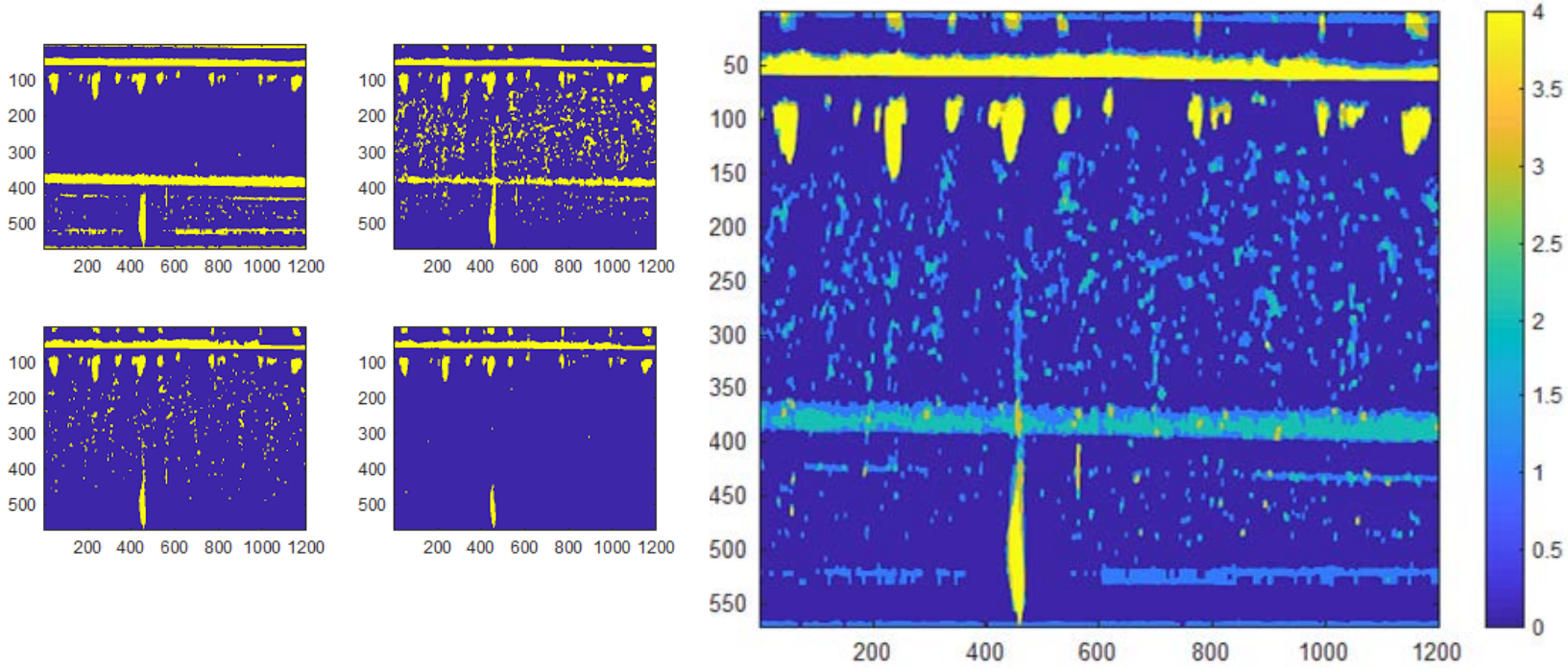

Morphologically filtered echograms (left), score matrix (right).

Region of Interest (ROI) extractor

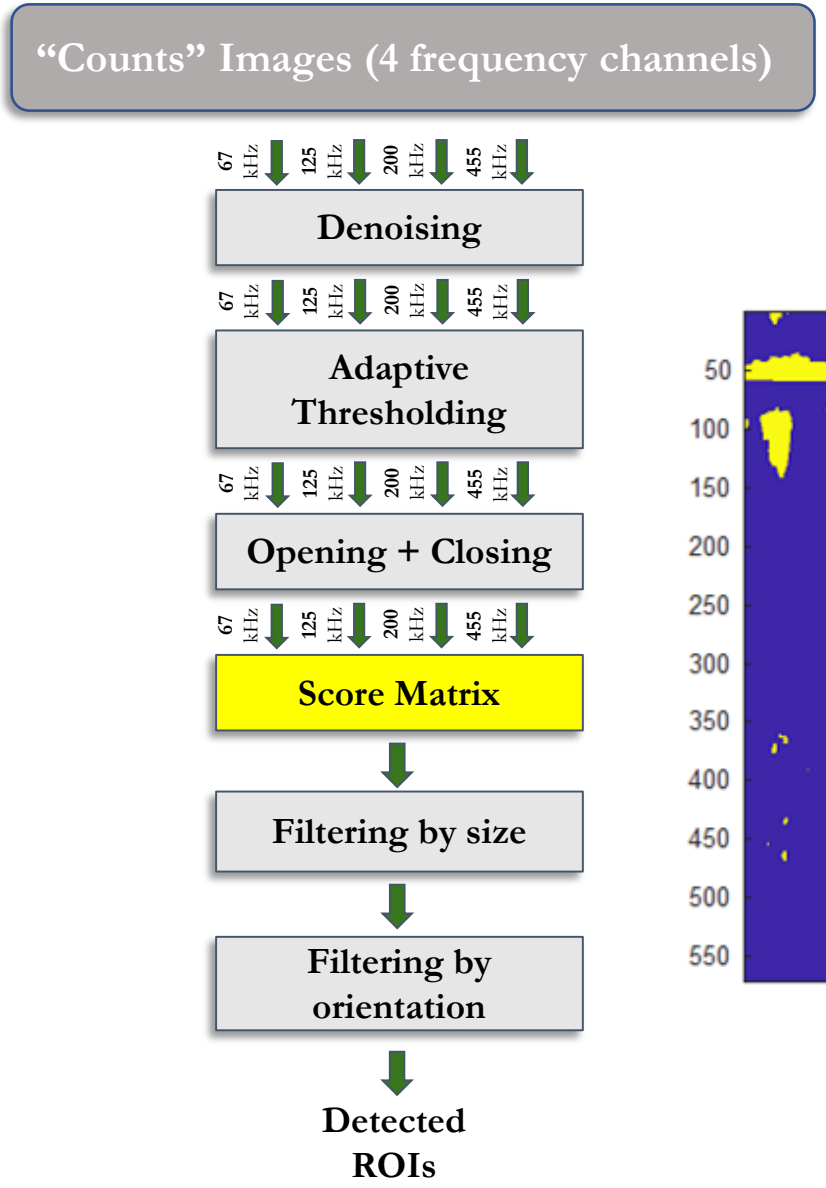

- Only positions with intensities > 2 are kept (i.e. signals present in three or more frequencies)

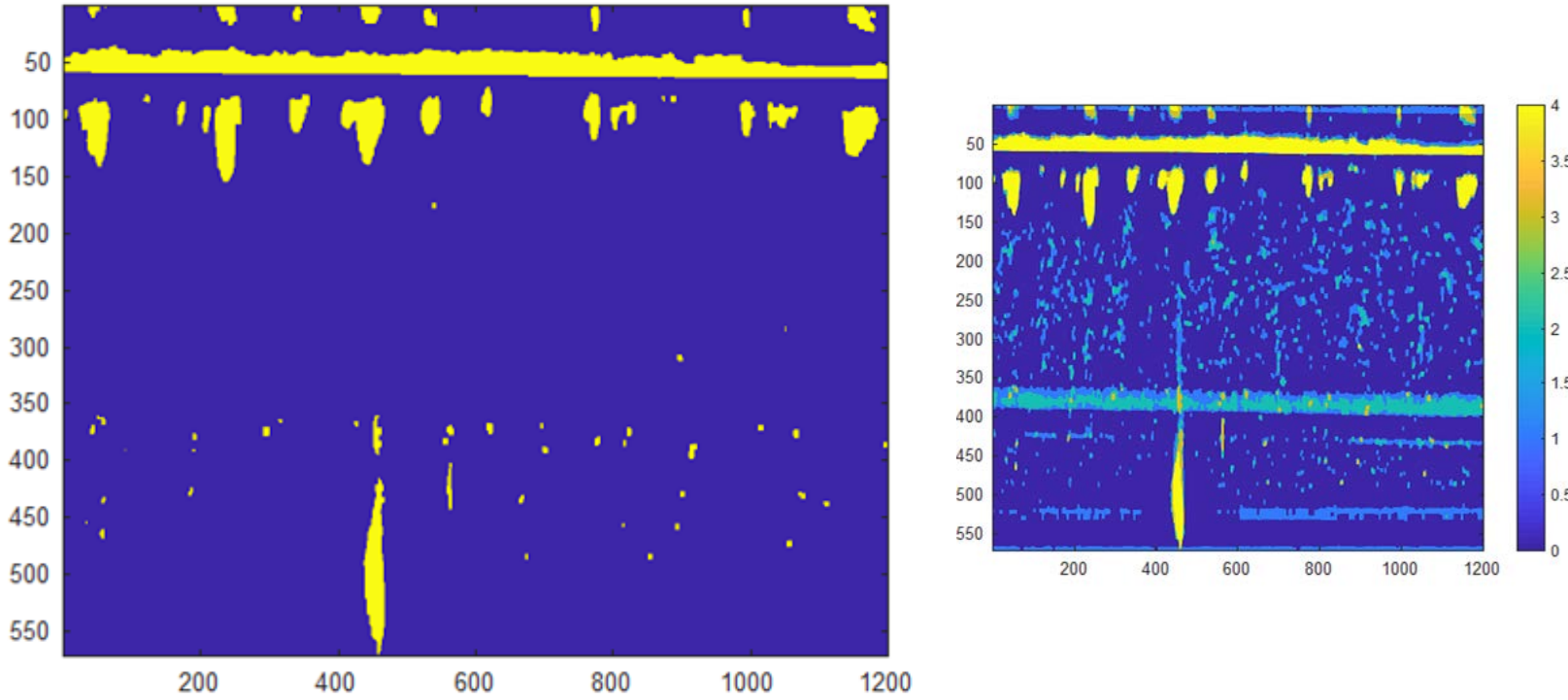

Filtered Score Matrix (left), unfiltered Score Matrix (right).

Region of Interest (ROI) extractor

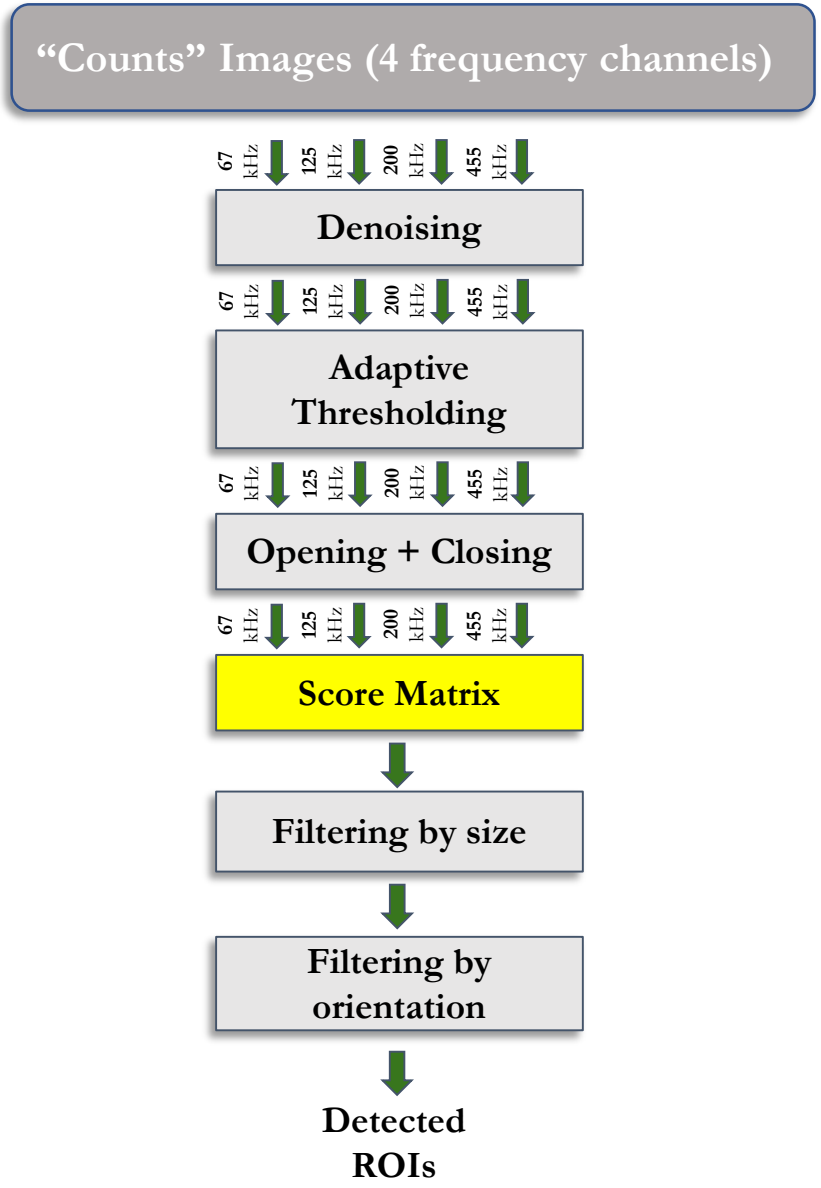

- Only positions with intensities > 2 are kept (i.e. signals present in three or more frequencies)

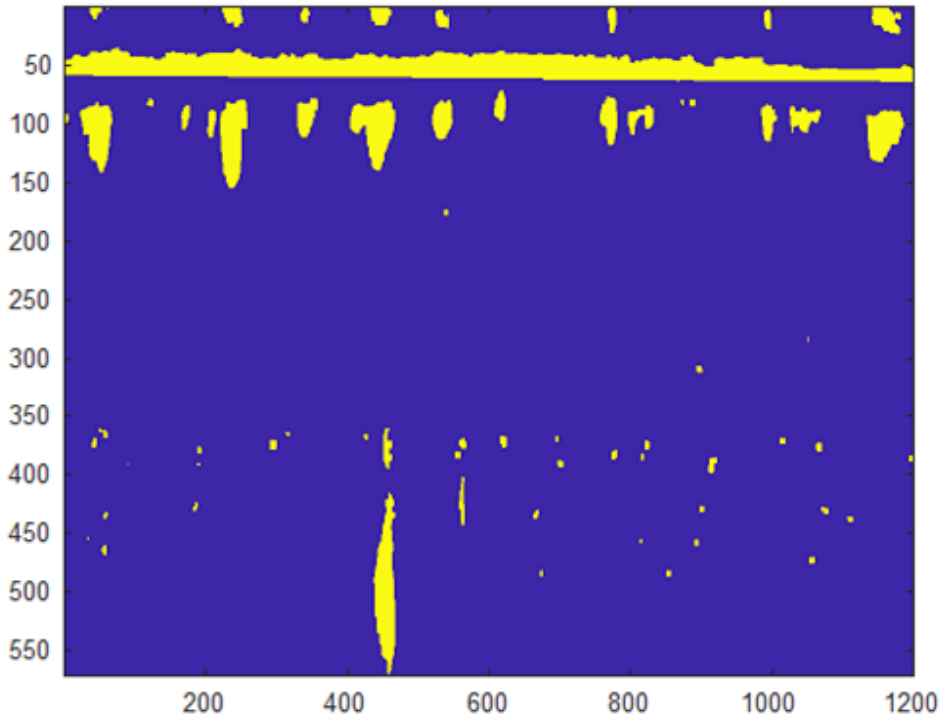

Filtered Score Matrix.

Region of Interest (ROI) extractor

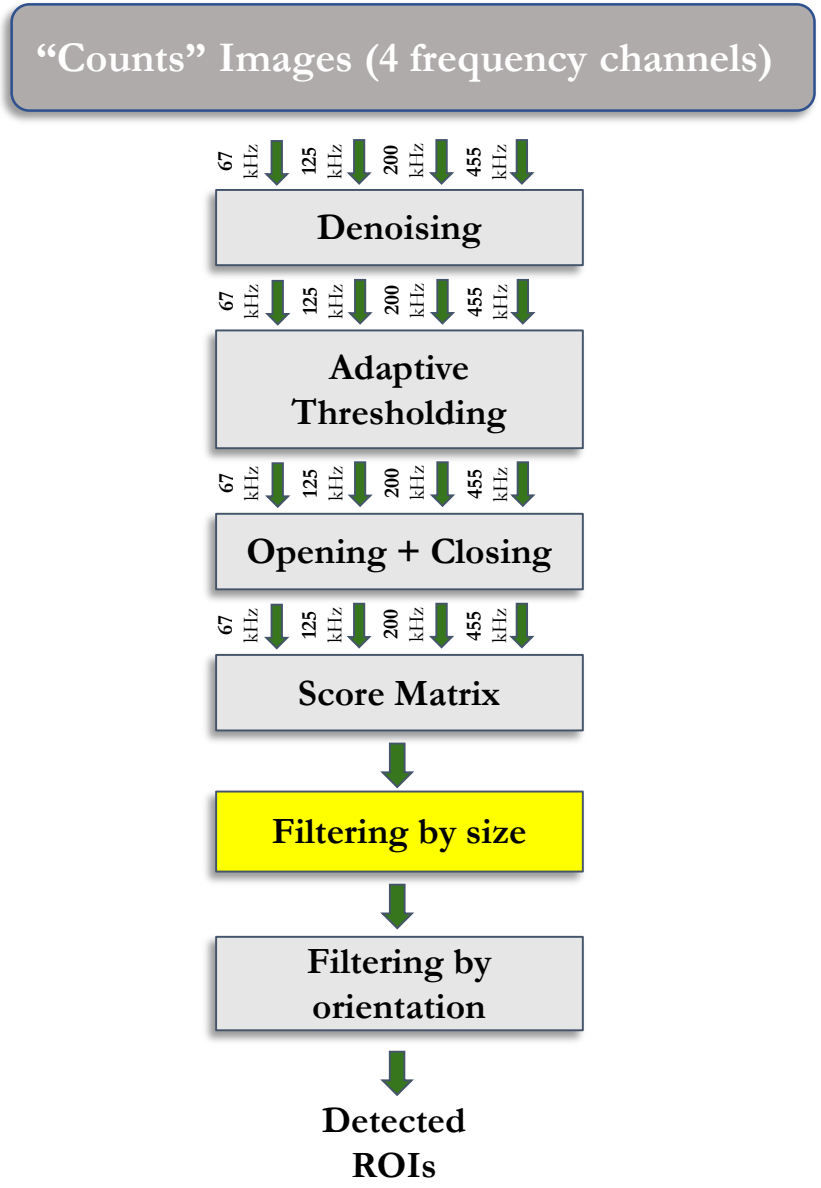

- Removes small acoustic responses (usually associated with individual fish)
- Threshold: 50 pixels

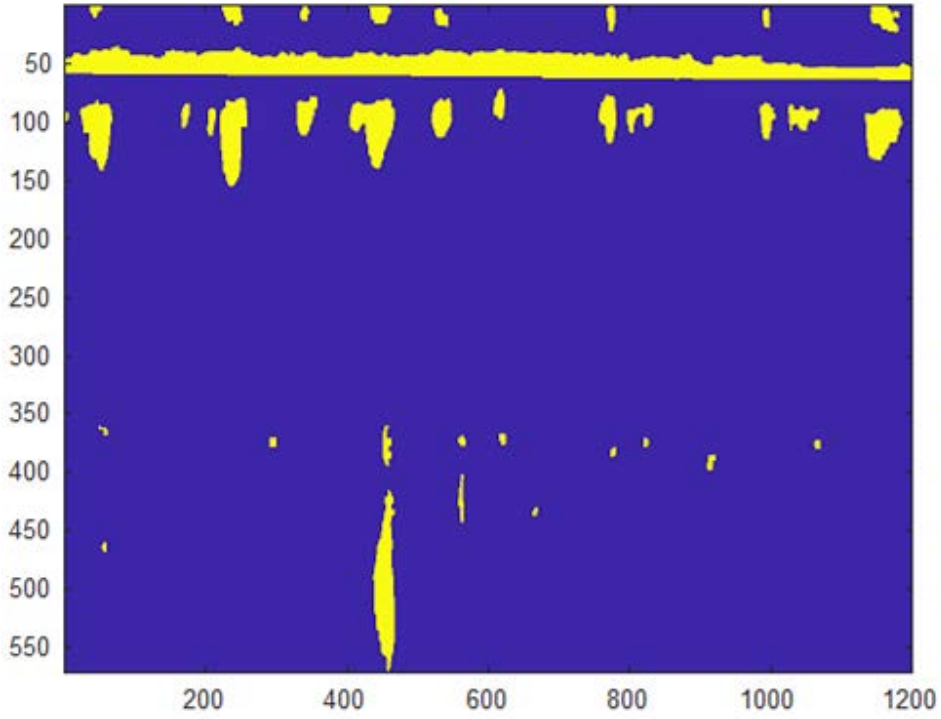

Output of size filtering step.

Region of Interest (ROI) extractor

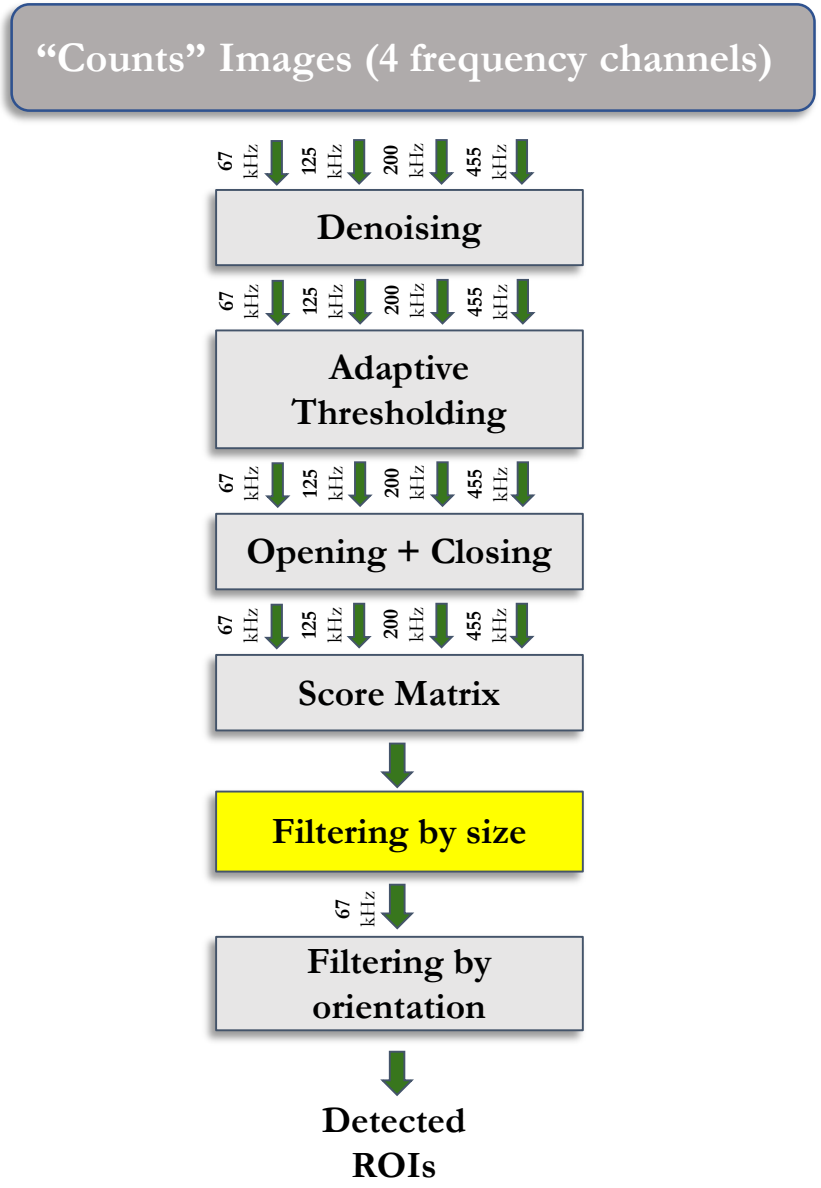

- Bounding boxes (BBs) around remaining structures.
- 67 kHz (more pronounced response for schools of herring)

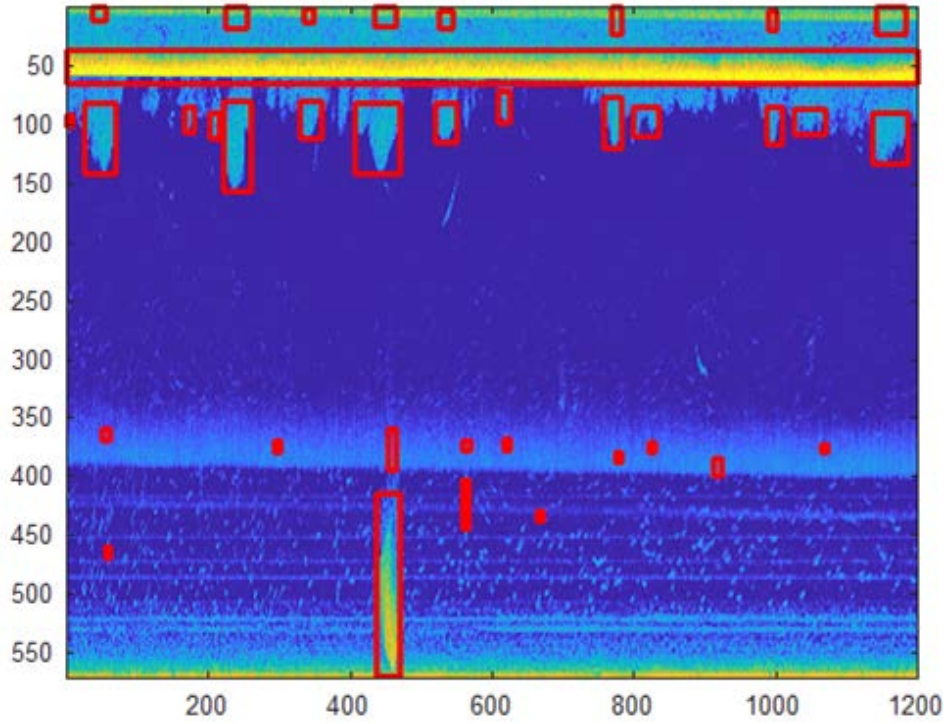

Initial bounding boxes.

Region of Interest (ROI) extractor

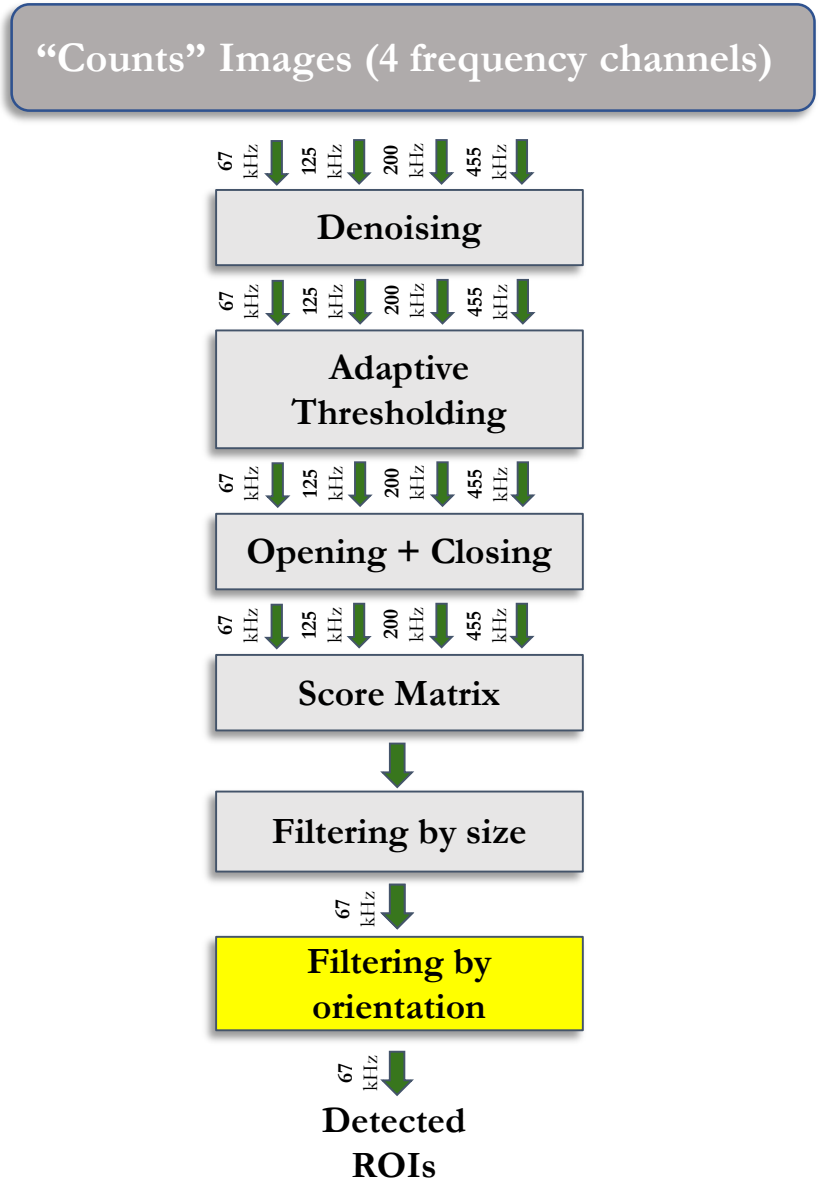

- Ignore a BB with $\alpha < 60°$
- **Contextual information about schools of herring**

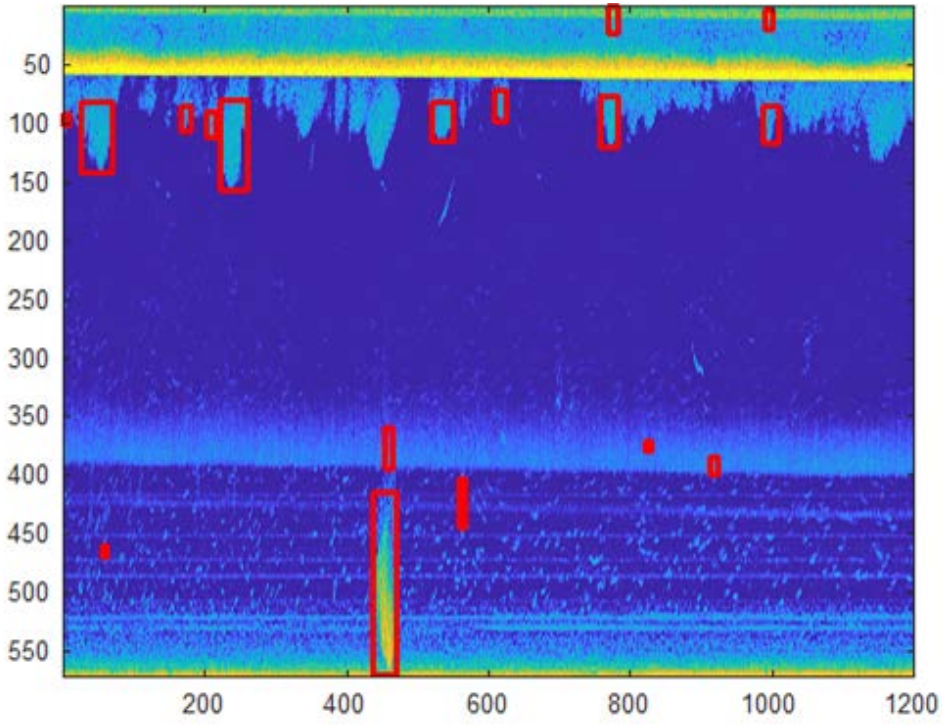

Output of BB orientation filtering (final ROIs).

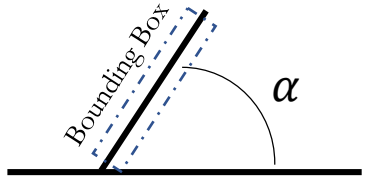

Region of Interest (ROI) extractor

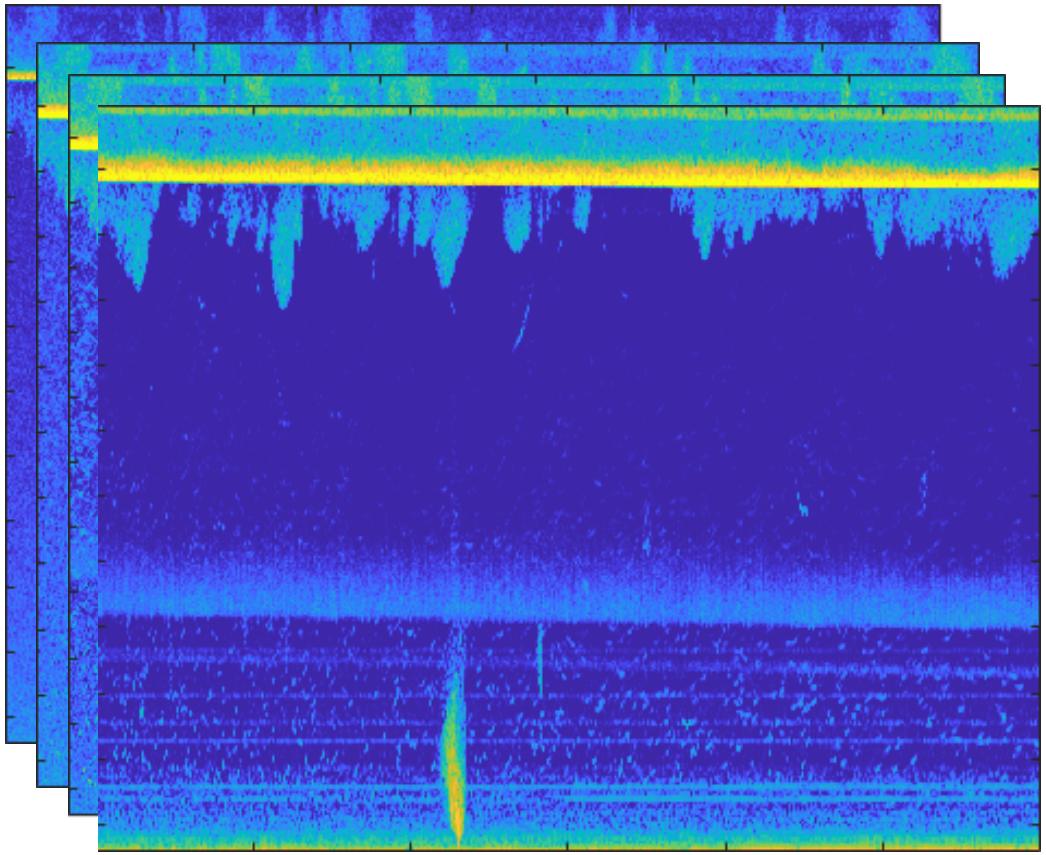

ROI extractor

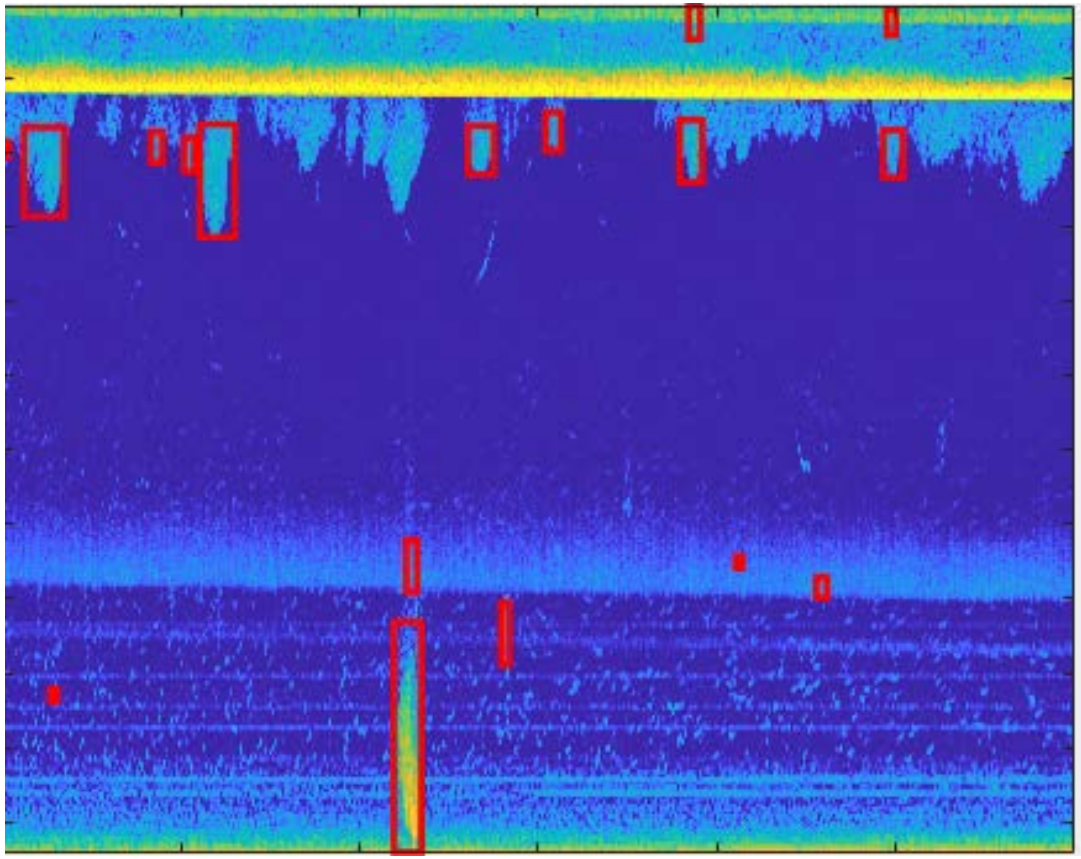

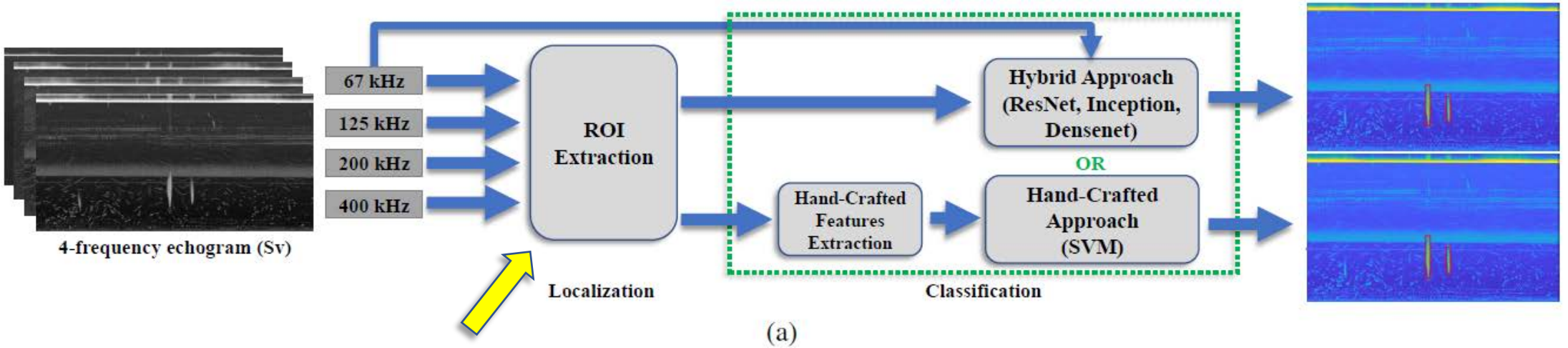

(a)

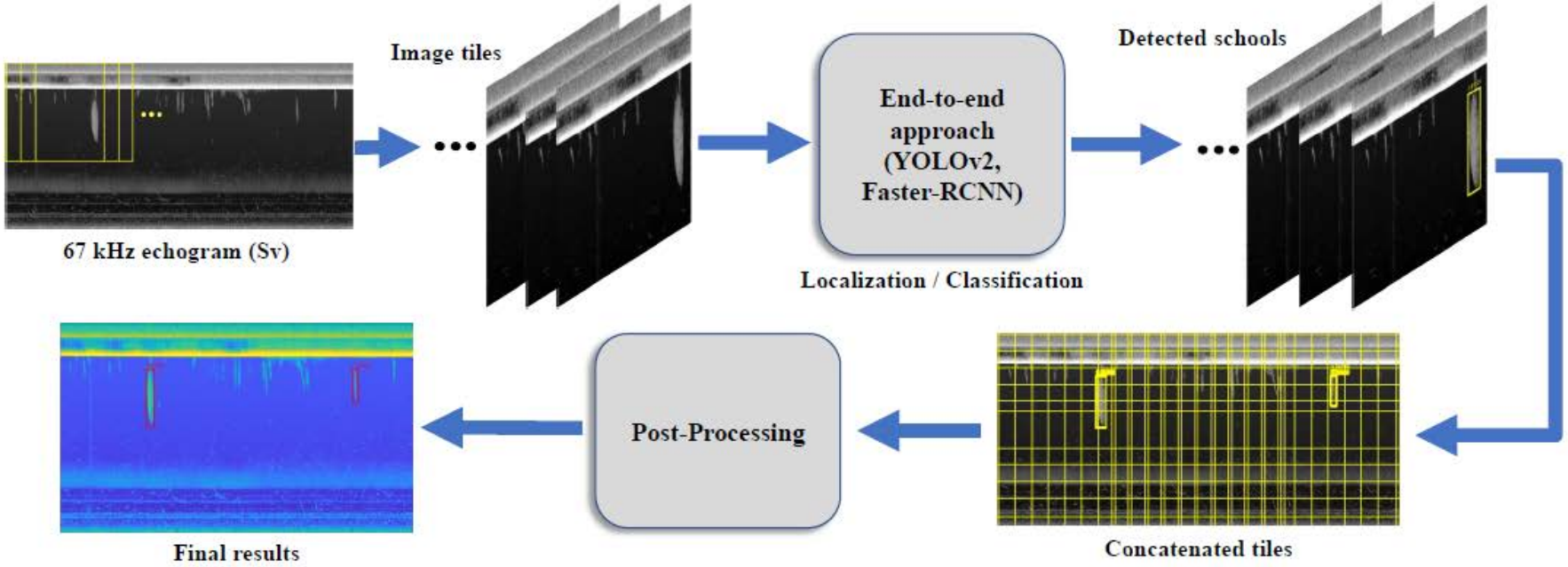

(b)

General block diagram of hand-crafted and hybrid approaches (a) and end-to-end approach (b). Red bounding boxes highlight the identified targets in the final results, shown on colour-coded echograms for better visualization.

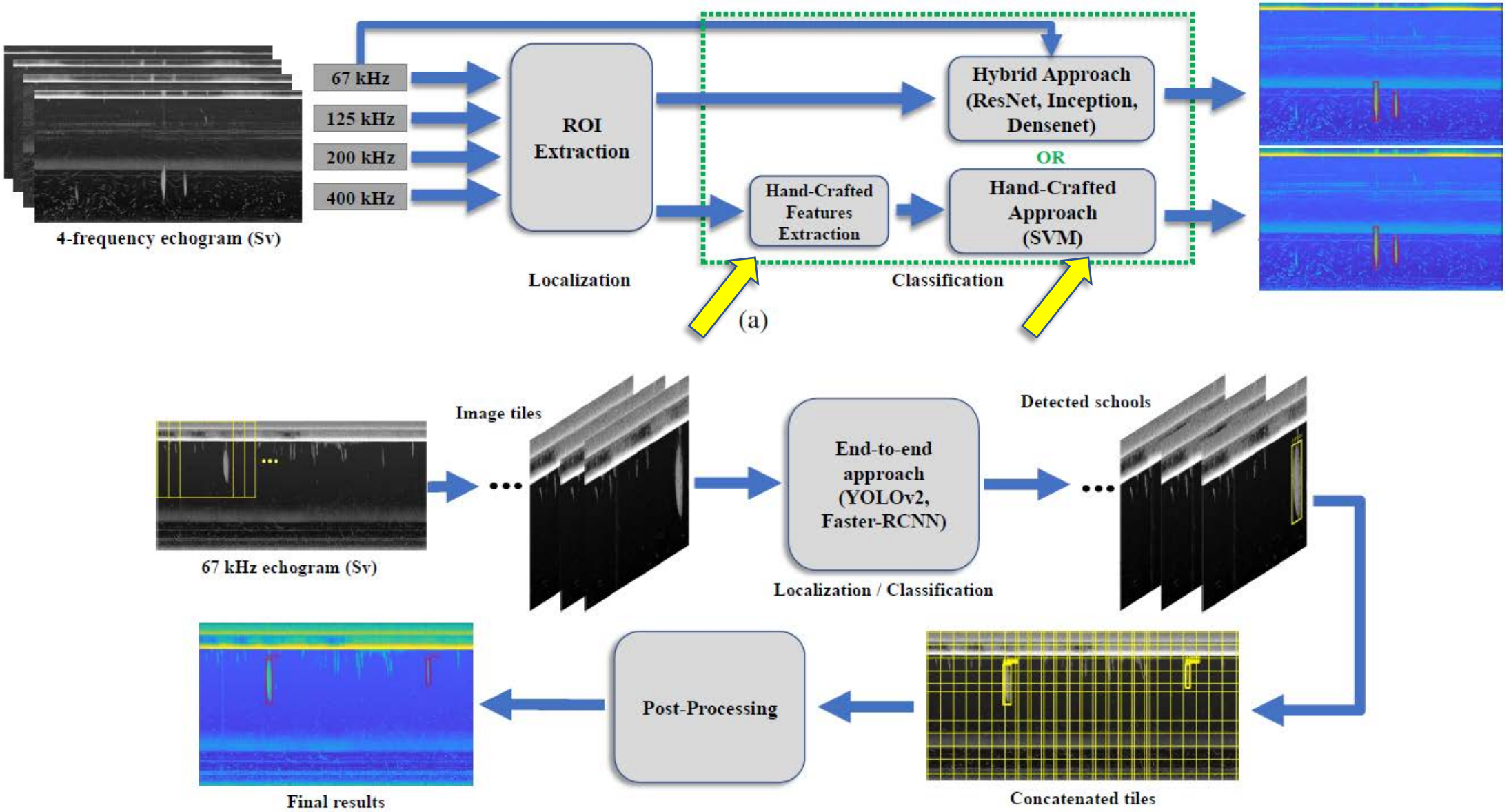

General block diagram of hand-crafted and hybrid approaches (a) and end-to-end approach (b). Red bounding boxes highlight the identified targets in the final results, shown on colour-coded echograms for better visualization.

Hand-crafted (SVM) approach

Output from the ROI extractor

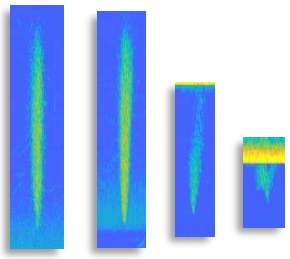

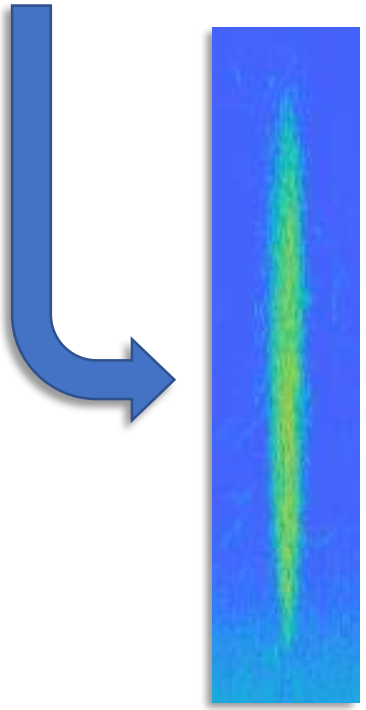

School of herring-specific features

Energetic

- Mean Intensity

Morphometric

- Ratio between major and minor axis
- Eccentricity
- Circularity

Custom-trained SVM classifier

Binary classification task

Classification Result: Herring / Background

Hand-crafted (SVM) approach

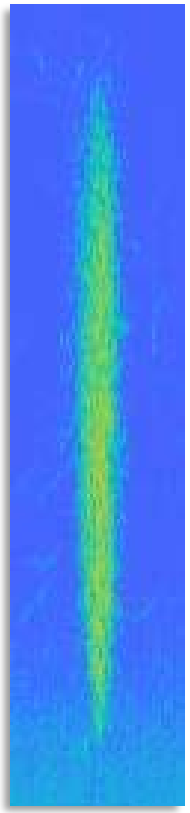

Herring

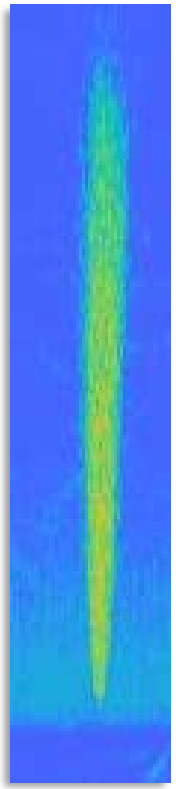

Herring

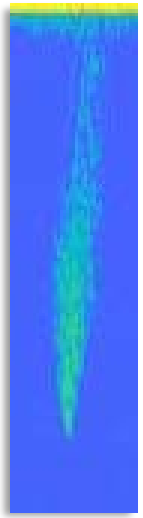

Background

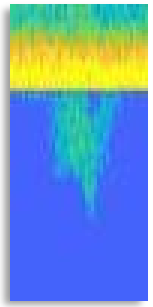

Background

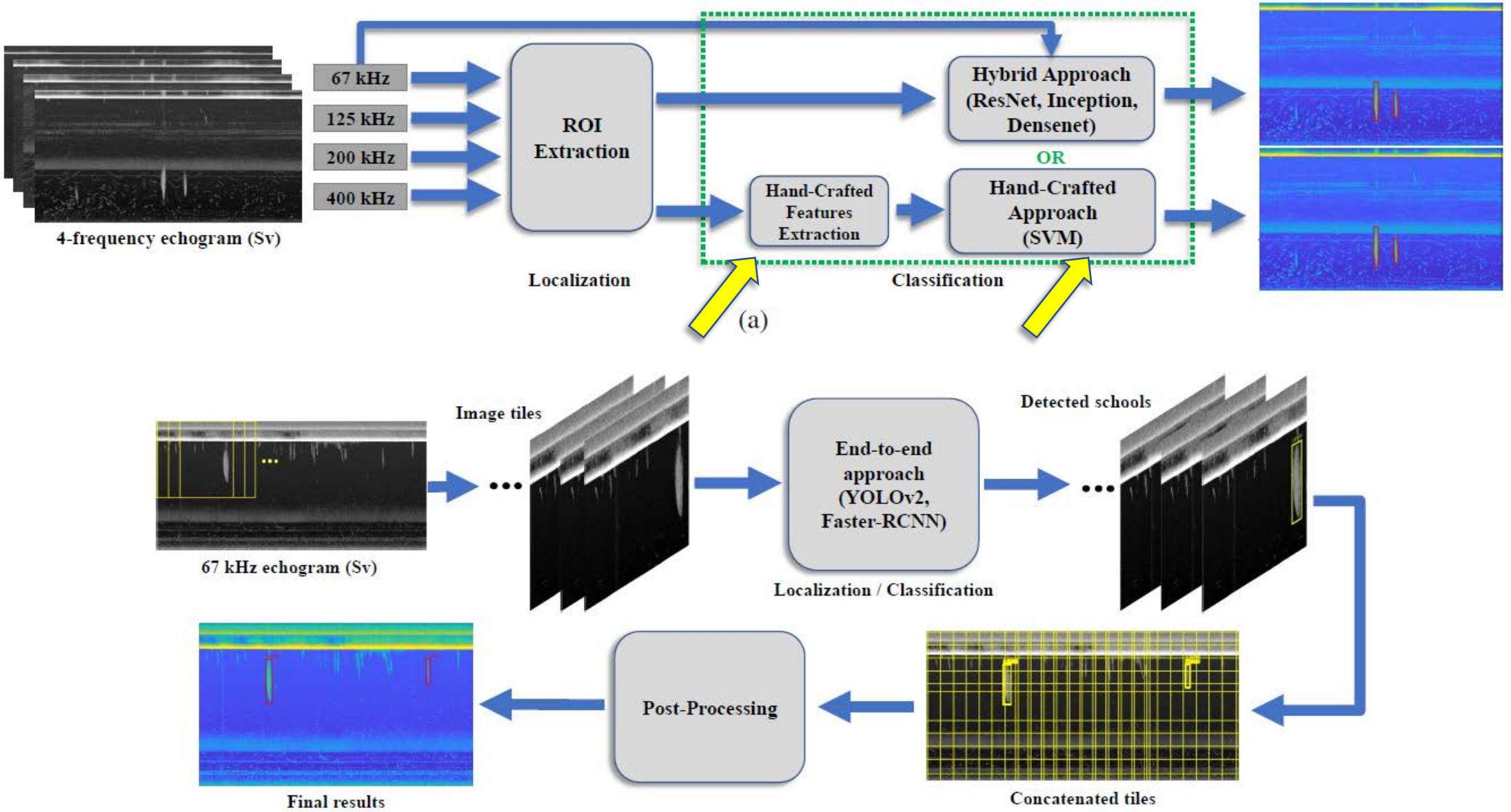

General block diagram of hand-crafted and hybrid approaches (a) and end-to-end approach (b). Red bounding boxes highlight the identified targets in the final results, shown on colour-coded echograms for better visualization.

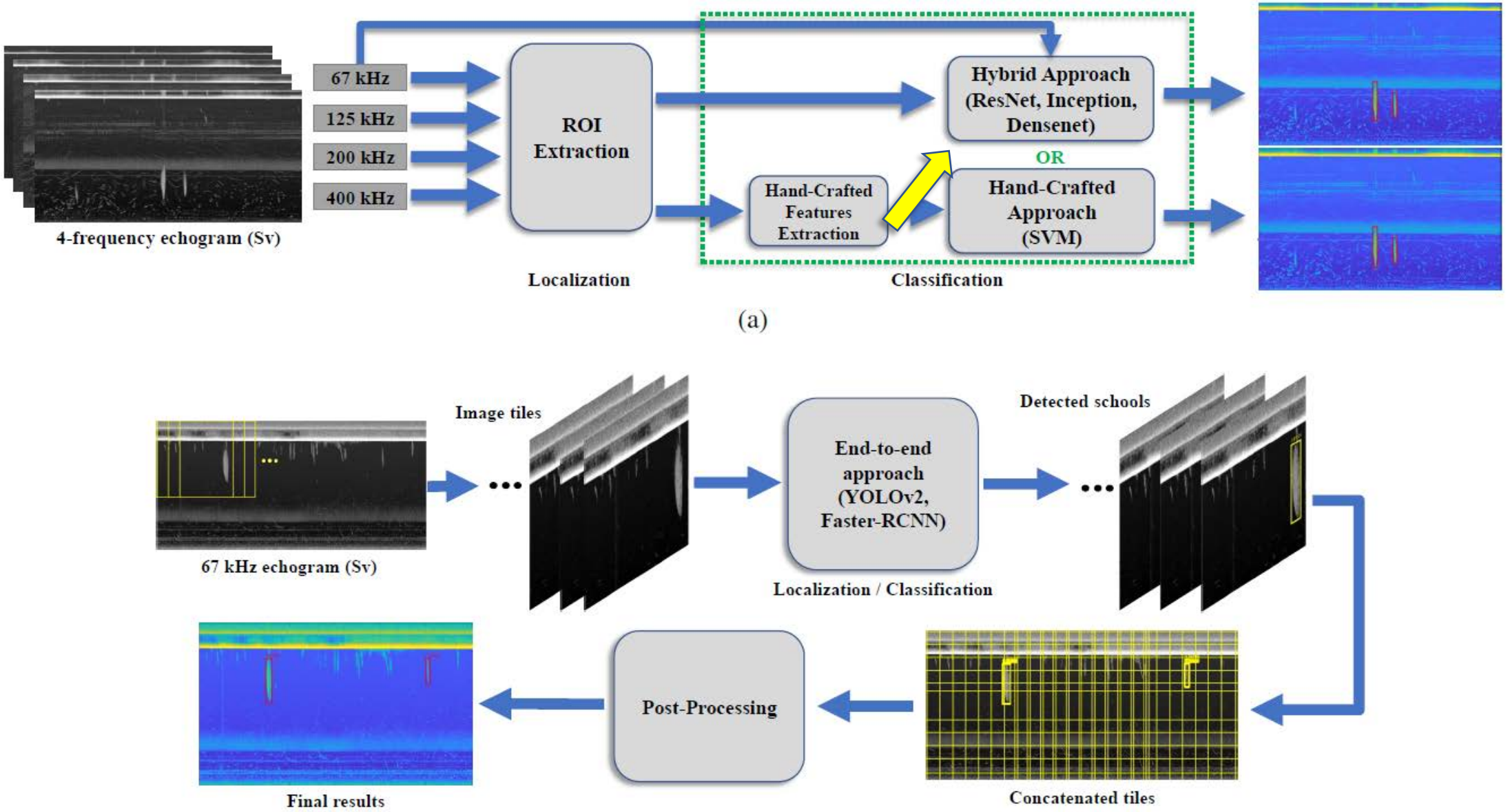

General block diagram of hand-crafted and hybrid approaches (a) and end-to-end approach (b). Red bounding boxes highlight the identified targets in the final results, shown on colour-coded echograms for better visualization.

Hybrid approach

Output from the ROI extractor

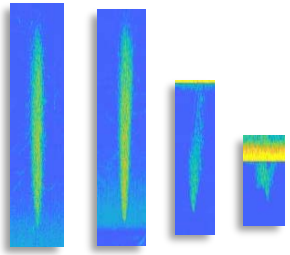

Trained with 286 echograms (total of 617 schools of herring)

Custom-trained image classifier

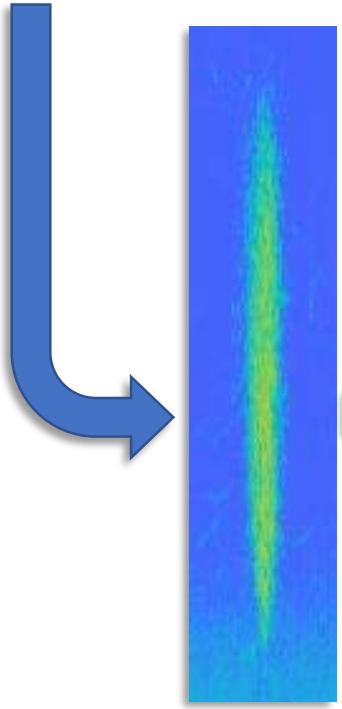

Feature extraction network (CNN-based)

ResNet-50 [22]
DenseNet-201 [23]
InceptionNetV3 [24]

Feature maps

Fully-Connected Layers

Neural Network

Binary classification task

Classification Result: Herring / Background

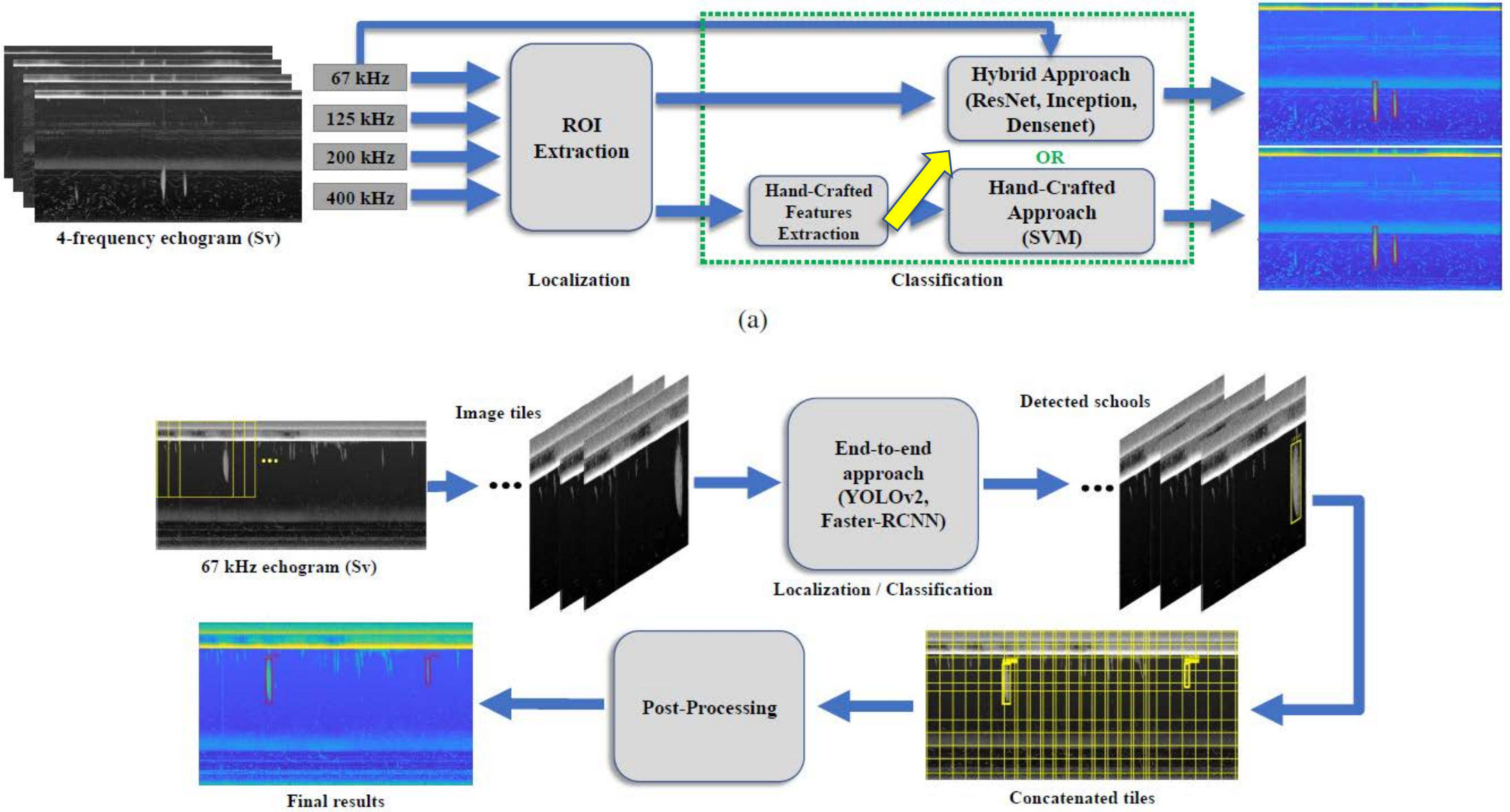

General block diagram of hand-crafted and hybrid approaches (a) and end-to-end approach (b). Red bounding boxes highlight the identified targets in the final results, shown on colour-coded echograms for better visualization.

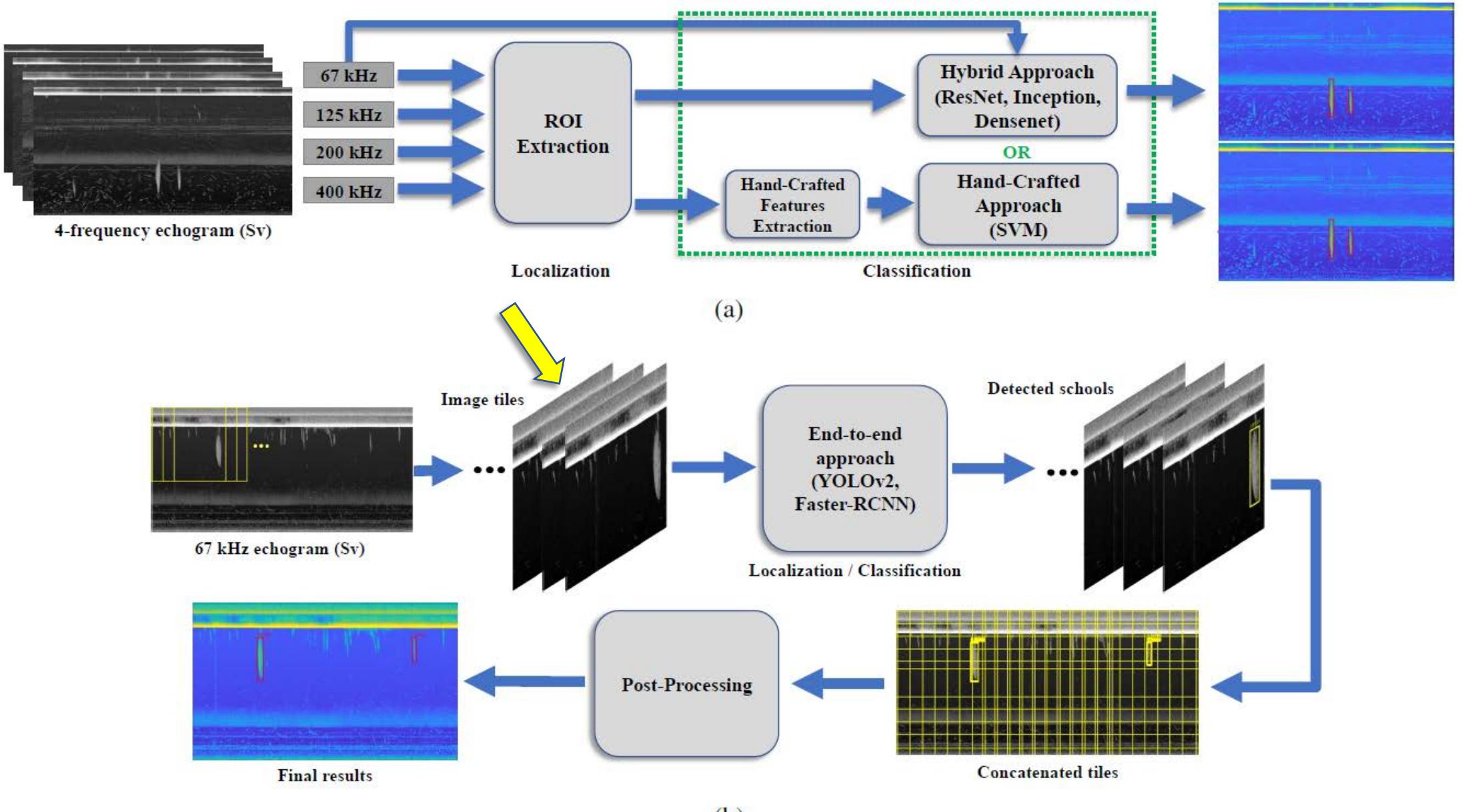

General block diagram of hand-crafted and hybrid approaches (a) and end-to-end approach (b). Red bounding boxes highlight the identified targets in the final results, shown on colour-coded echograms for better visualization.

End-to-end approach: scale issue

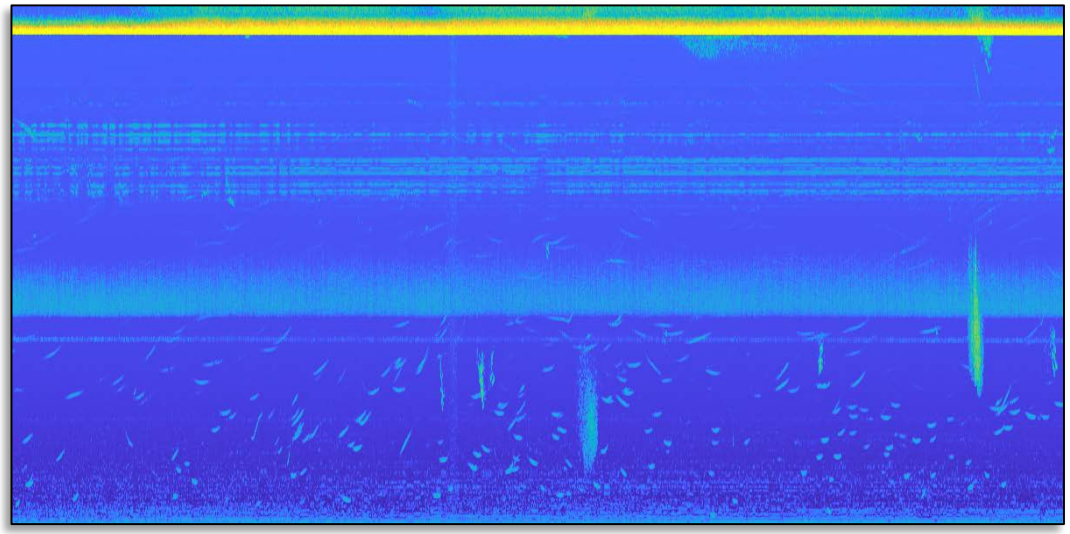

End-to-end approach: scale issue

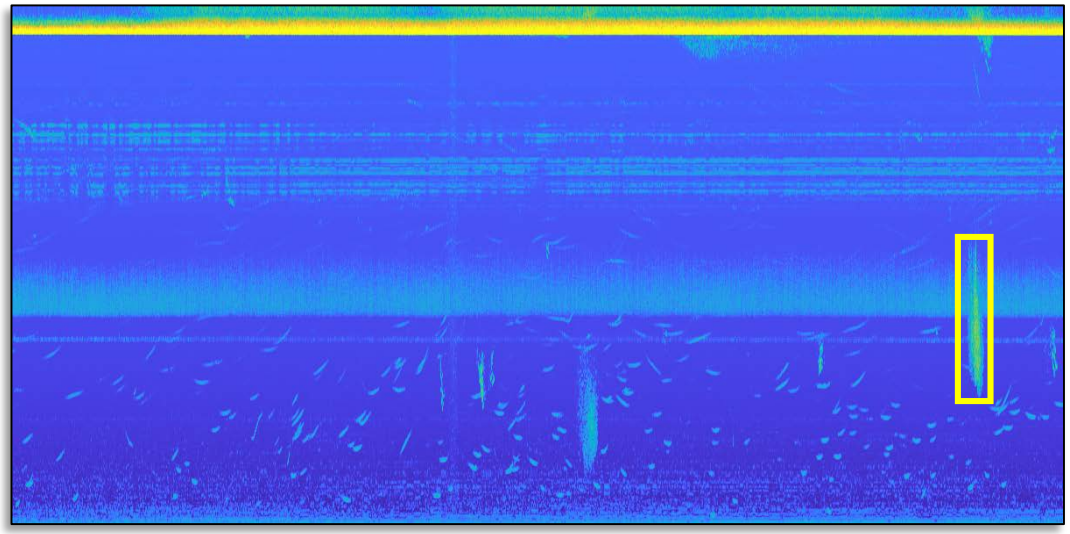

Scale **a**

End-to-end approach: scale issue

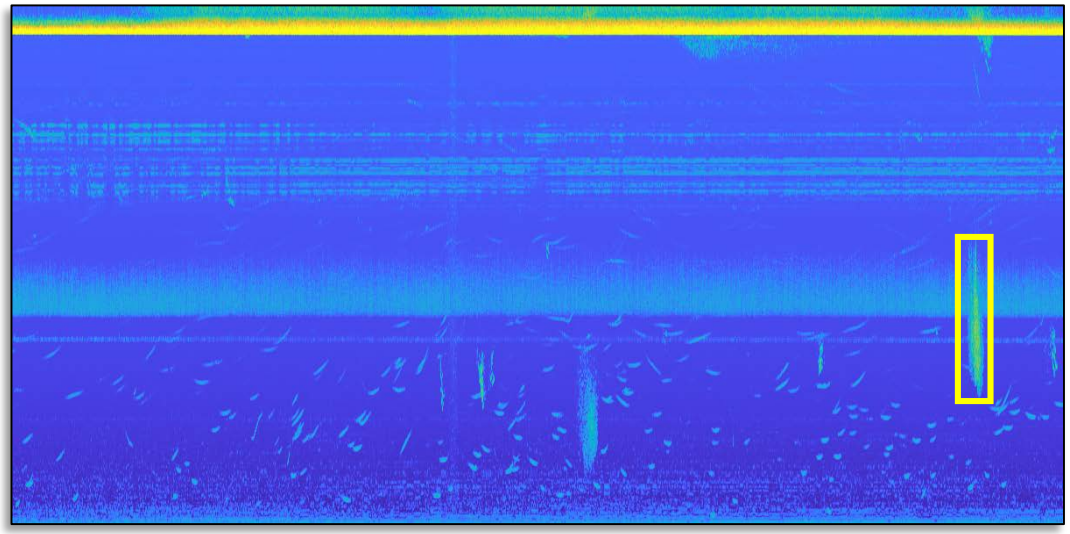

Scale **a**

Resizing

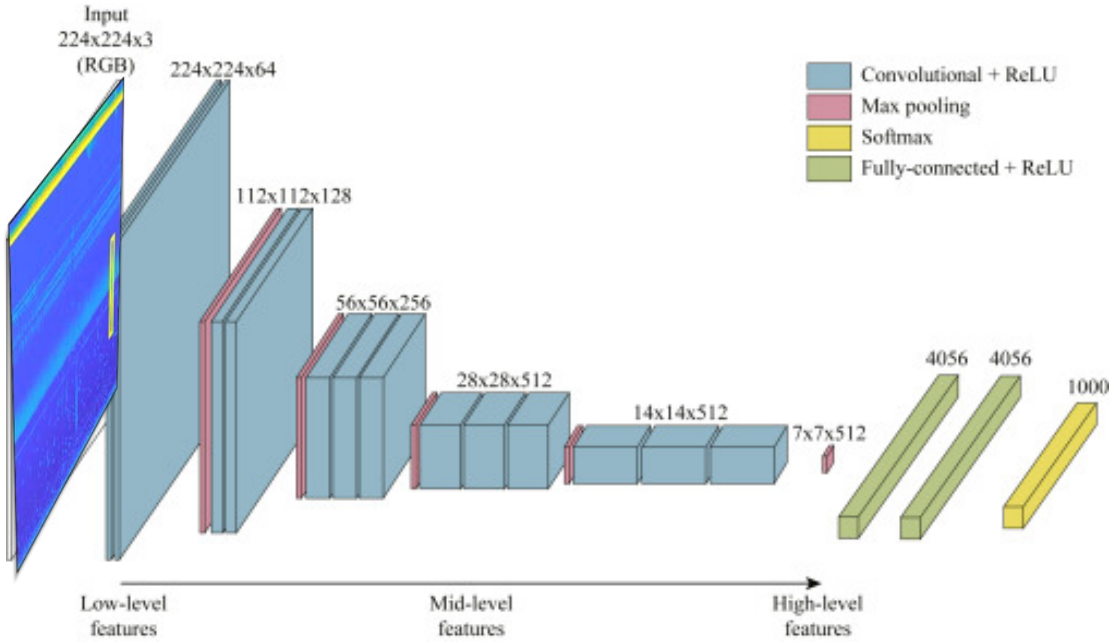

A generic convolution-based feature extractor (adapted from Pinaya et al., 2020).

Pinaya, W. H. L. et al. *Machine Learning: Methods and Applications to Brain Disorders*. Academic Press, 2020, pp. 173-191.

End-to-end approach: scale issue

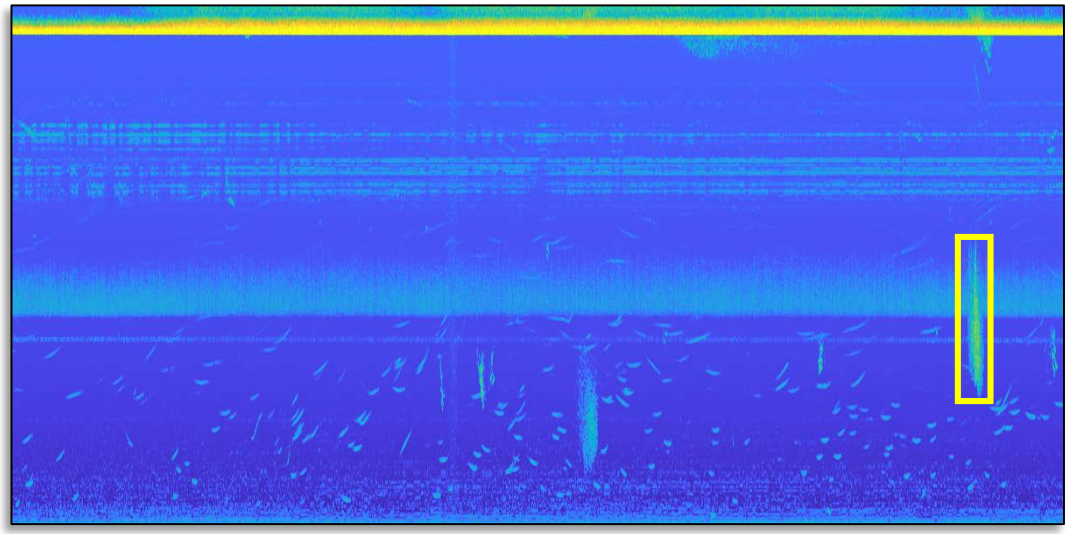

Scale **a** >>> Scale **b**

Resizing

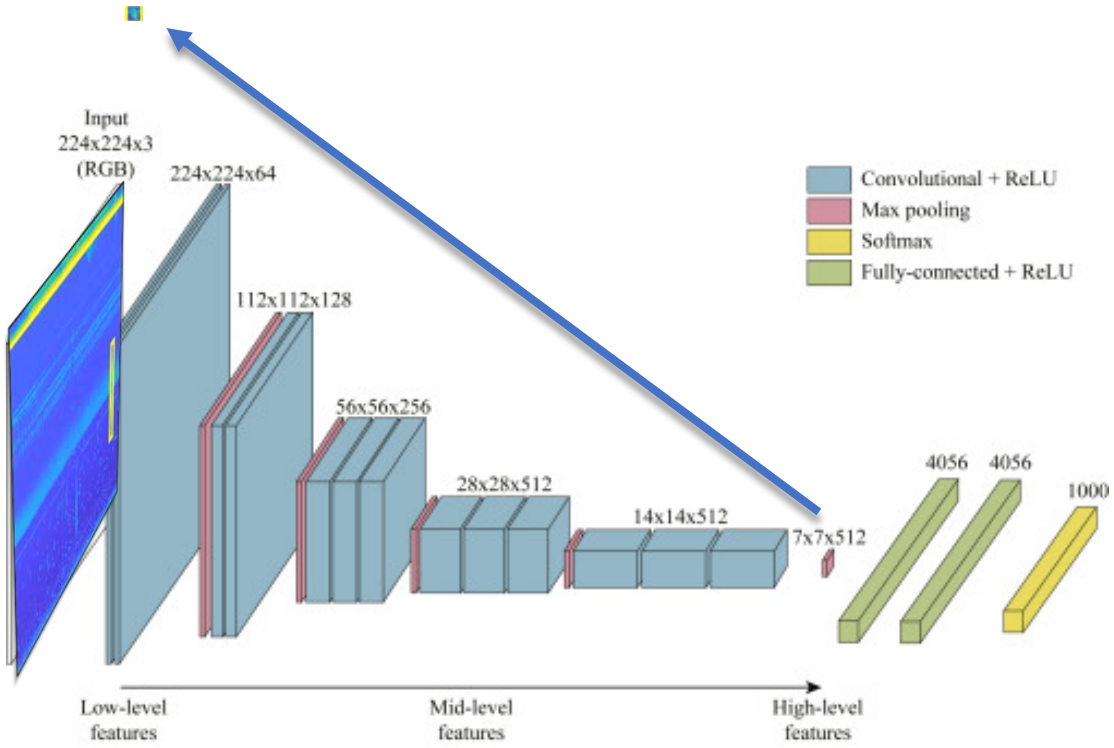

A generic convolution-based feature extractor (adapted from Pinaya et al., 2020).

Pinaya, W. H. L. et al. *Machine Learning: Methods and Applications to Brain Disorders*. Academic Press, 2020, pp. 173-191.

Tiling strategy

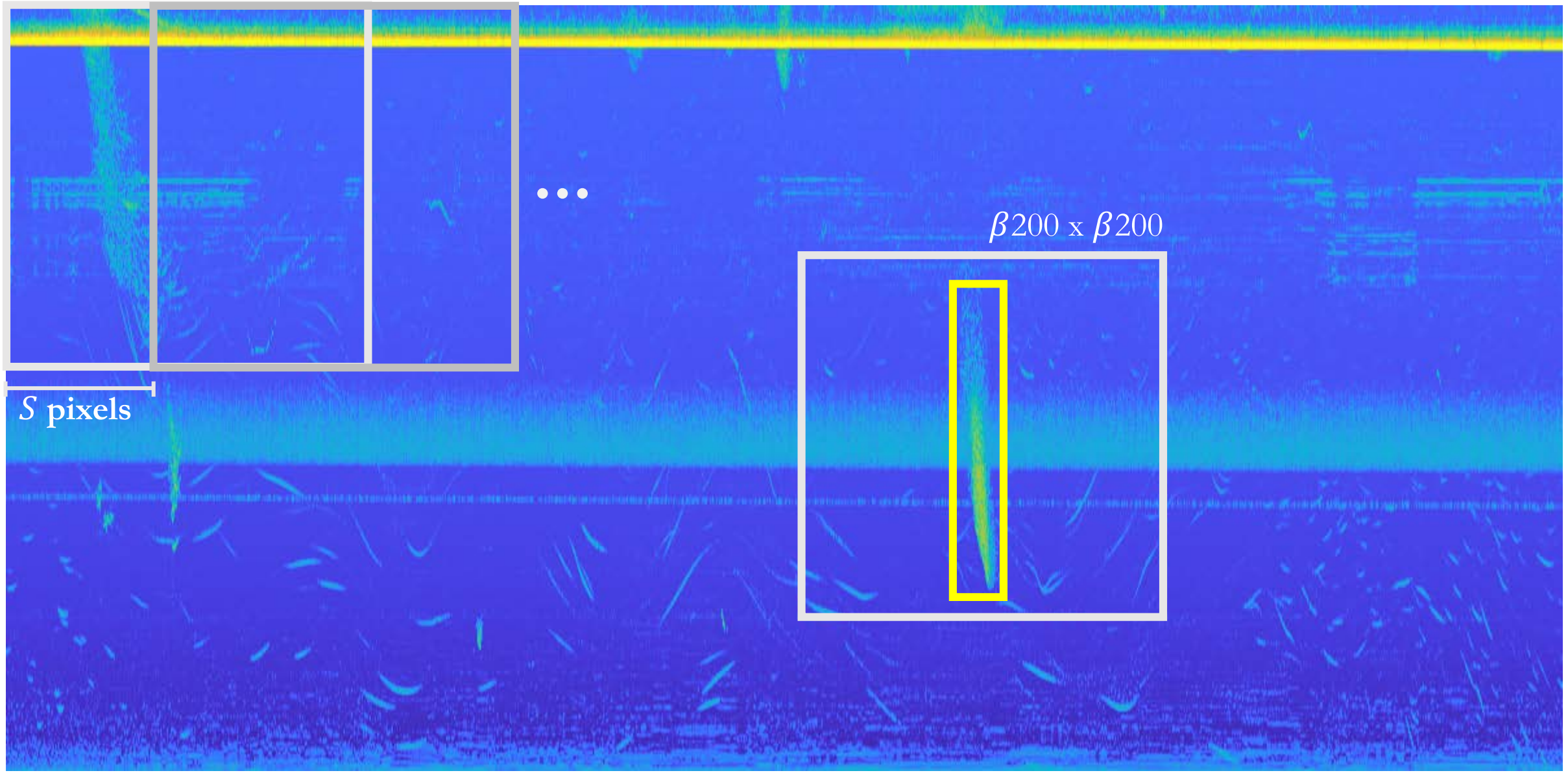

Tiling strategy

224x224

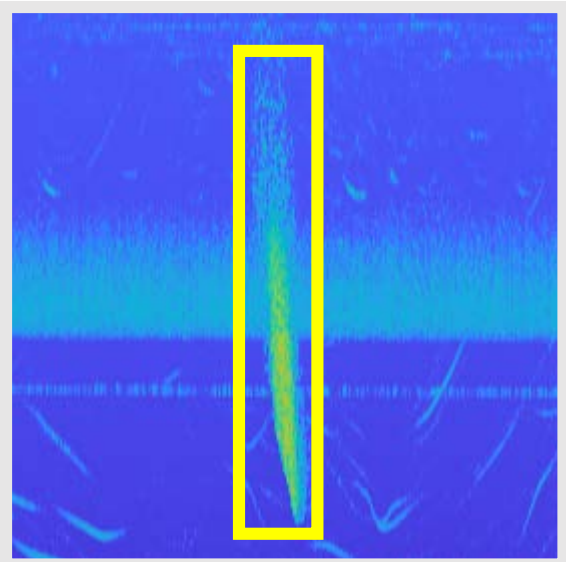

No resizing

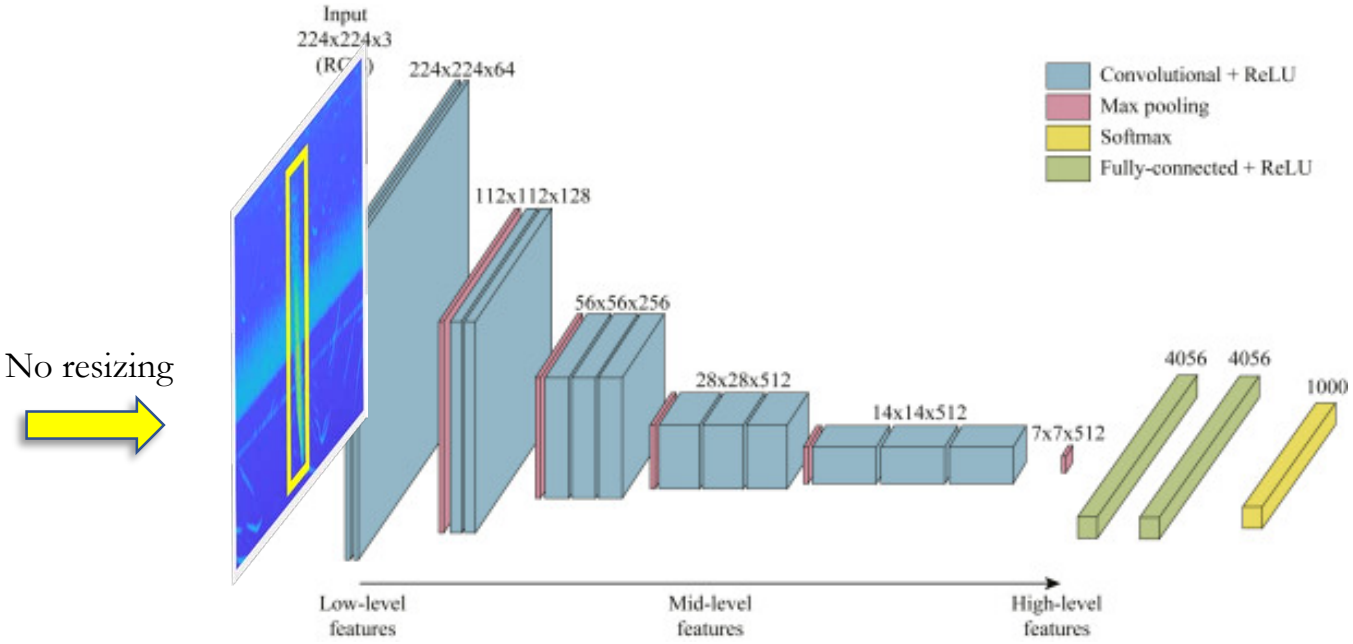

A generic convolution-based feature extractor (adapted from Pinaya et al., 2020).

Pinaya, W. H. L. et al. *Machine Learning: Methods and Applications to Brain Disorders*. Academic Press, 2020, pp. 173-191.

Tiling strategy

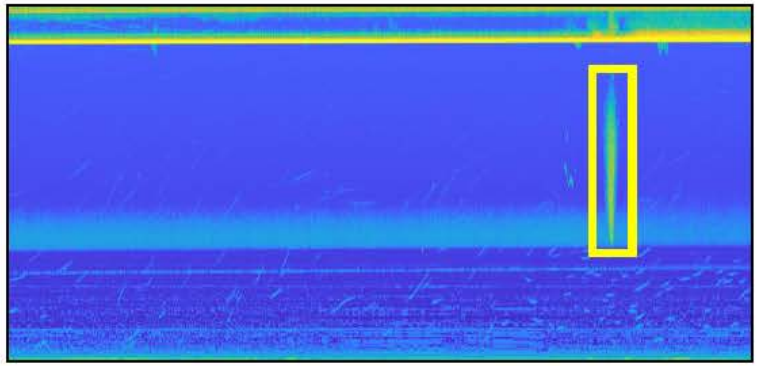

(a) Original echogram

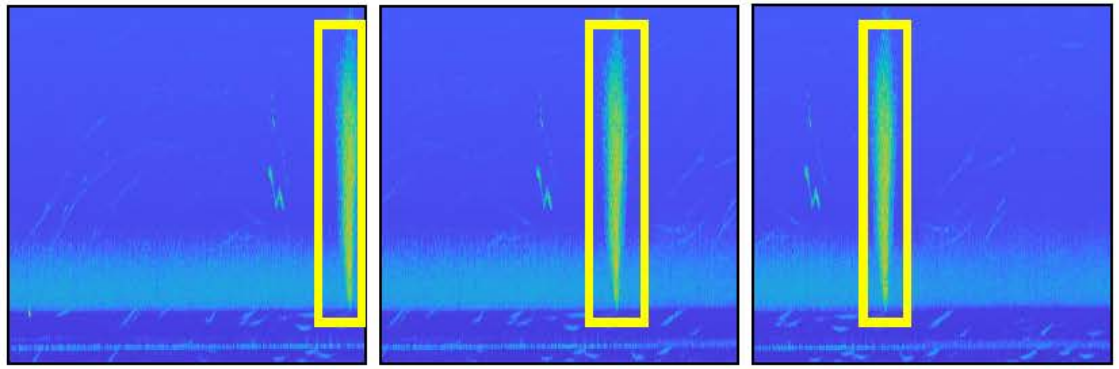

(b) Three overlapping tiles

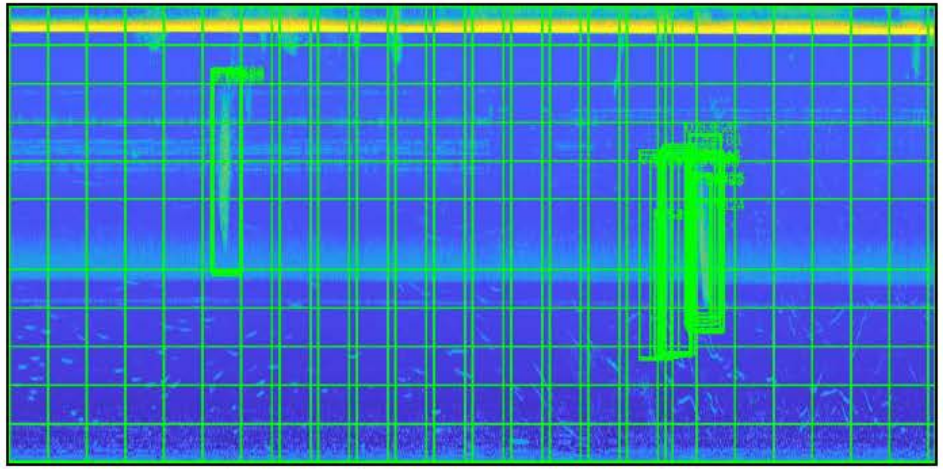

(c) Multiple detection (inference)

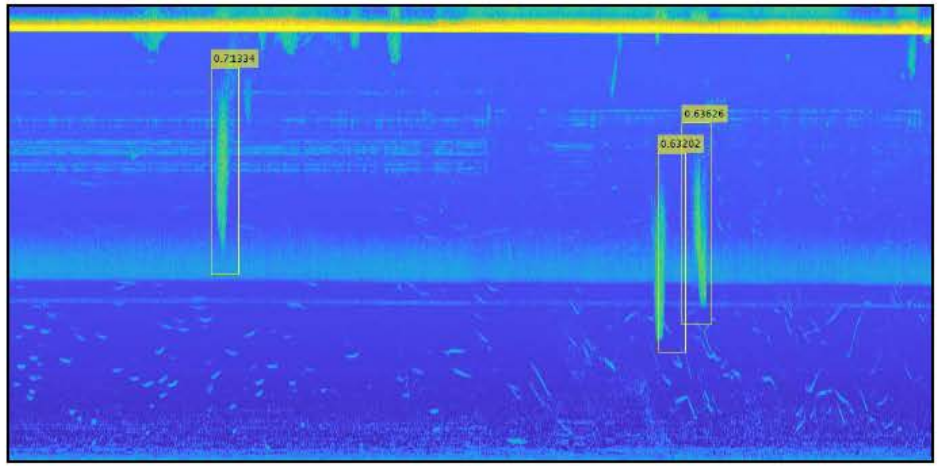

(d) Concatenated detection results

Tiling strategy used for training and inference. Original echogram (571x1200) with ground truth annotation highlighted in yellow (a). Tiles of 340x340 created around the annotation for the training phase, highlighted in yellow (b). Multiple tiles (green), with the first tile highlighted in black, and individual detection results (red bounding boxes) obtained during inference (c). Detection bounding boxes (red) obtained after post-processing (d).

Dataset

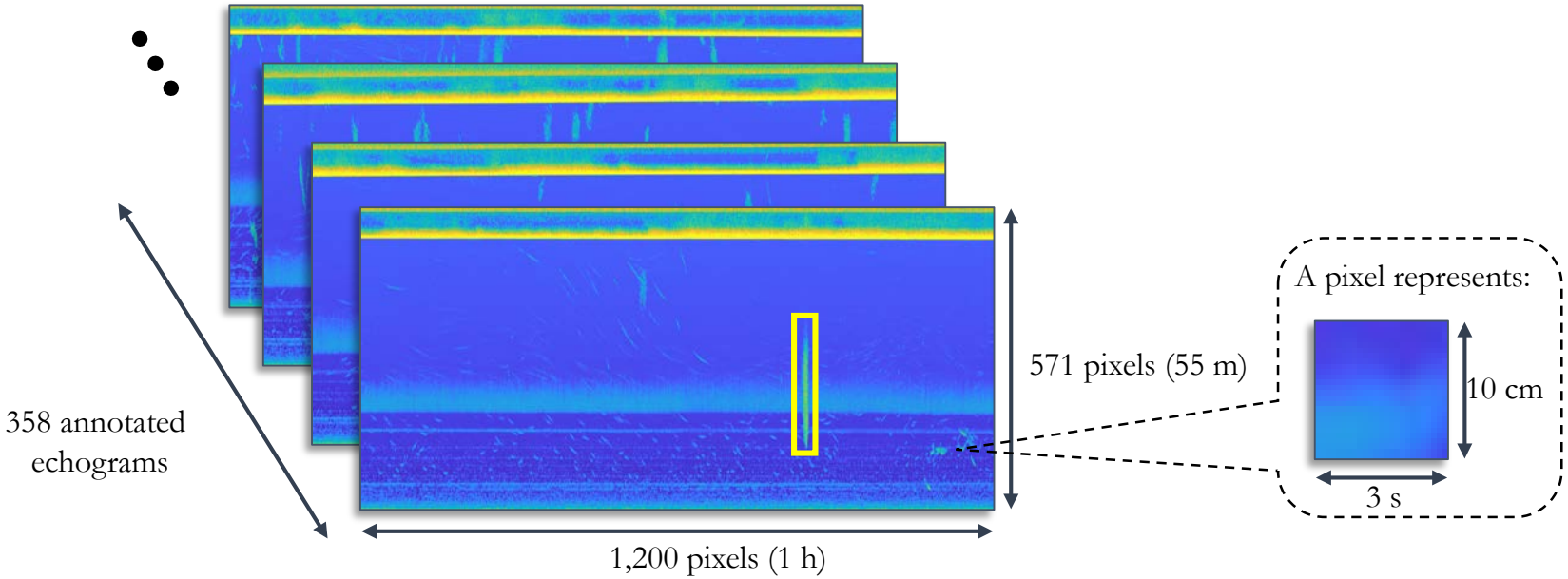

- Canada's Department of Fisheries and Oceans (DFO)
- ASL Environmental Sciences' AZFP [1] echosounder
- Okisollo channel, BC, Canada
- May - October 2015 and 2016

Dataset

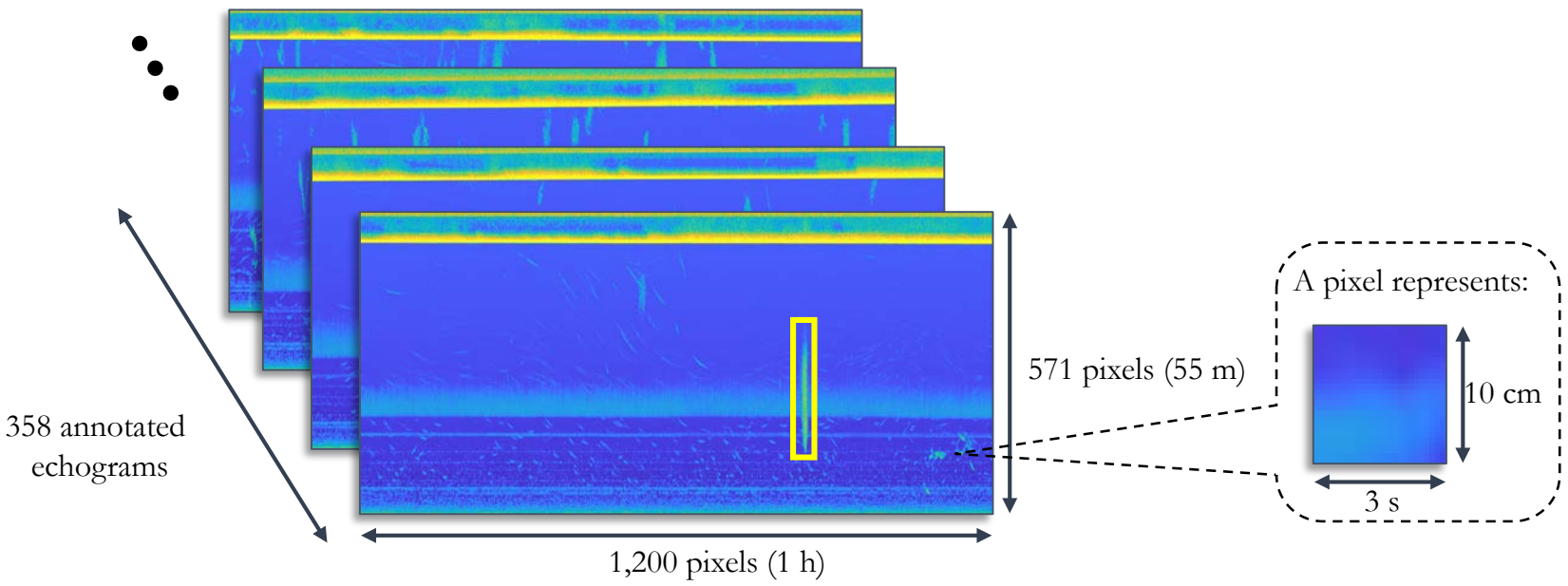

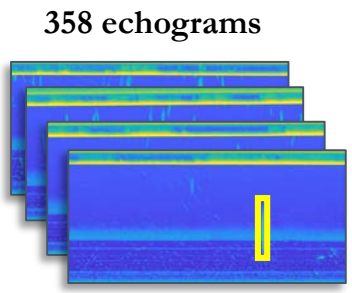

- Canada's Department of Fisheries and Oceans (DFO)
- ASL Environmental Sciences' AZFP [1] echosounder
- Okisollo channel, BC, Canada
- May - October 2015 and 2016

80%
Training/validation

- 286 echograms
- 617 instances of schools of herring
- Tiles for the end-to-end approach

20%
Testing

- 72 echograms
- 128 instances of schools of herring

Ground truth

Detection

Qualitative results

1) Hand-crafted (SVM)

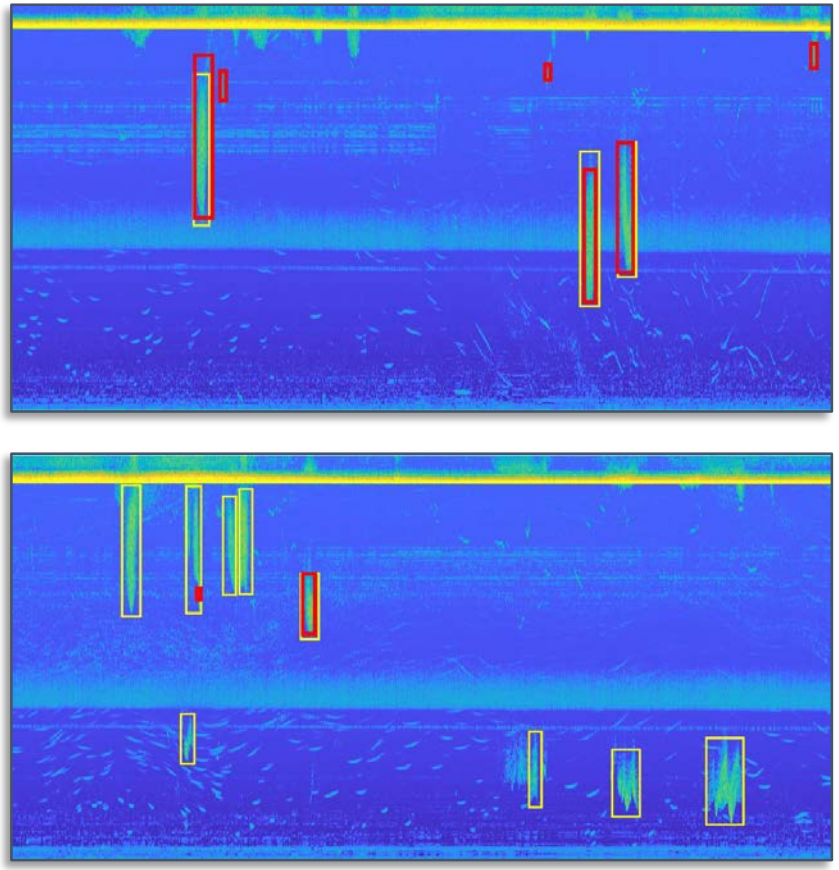

2) Hybrid (InceptionV3 [24])

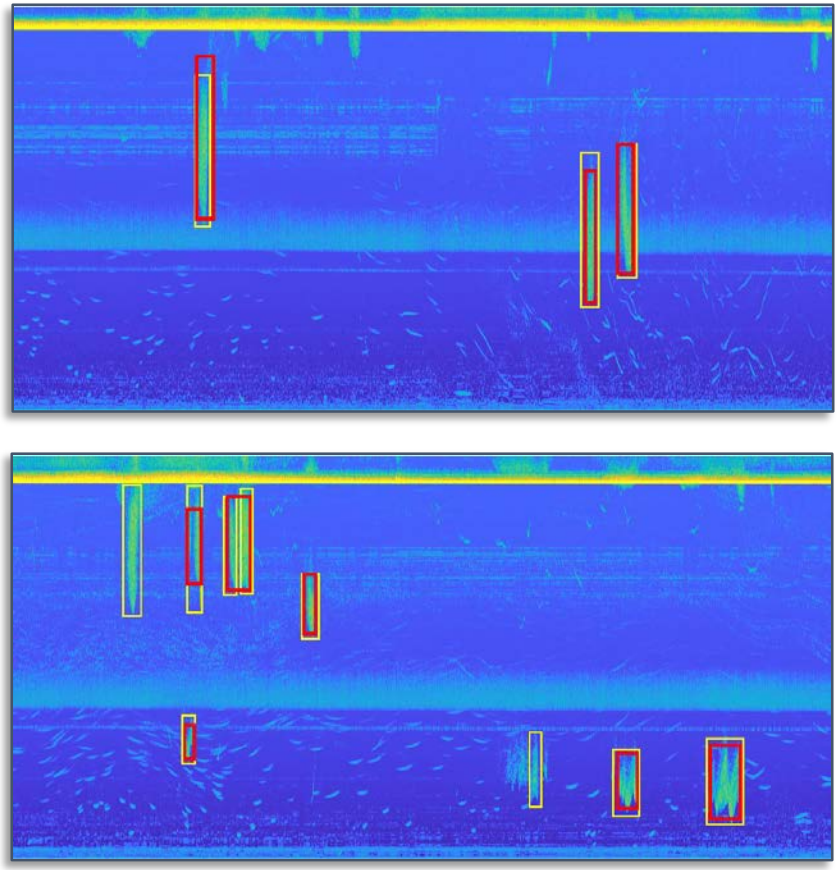

3) End-to-end (YOLOv2 [26])

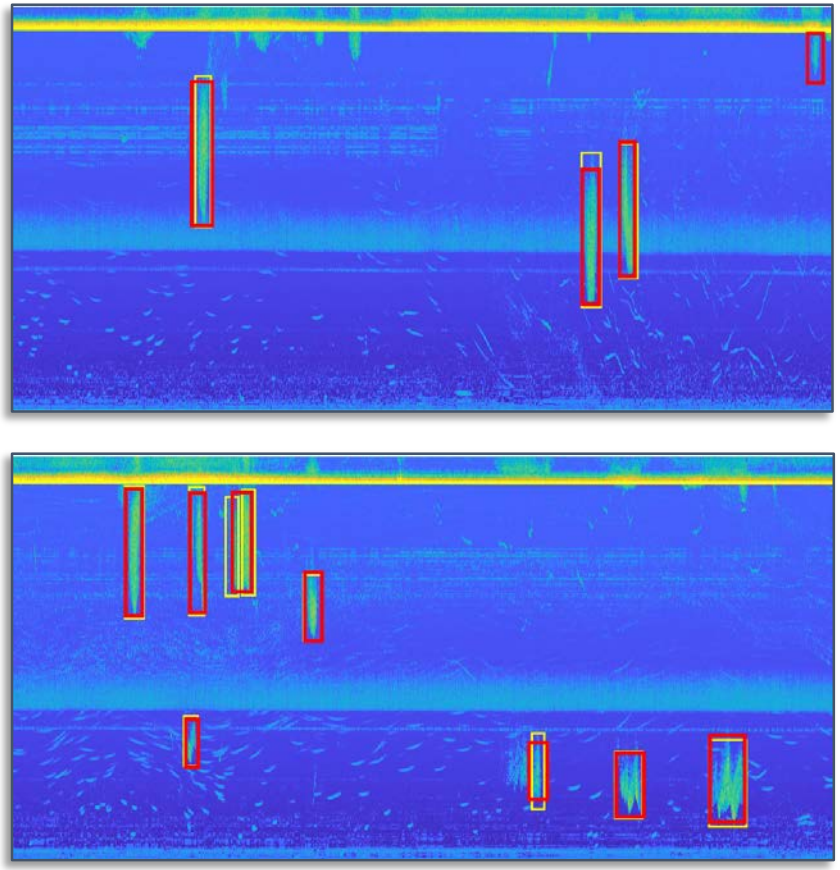

Quantitative results

Method	IoU	P	R	F1
1) Hand-crafted (SVM [29])	0.3	45.41	65.63	53.67
1) Hand-crafted (SVM [29])	0.5	41.62	60.16	49.20
2) Hybrid (ResNet-50 [22])	0.3	72.37	85.94	78.57
2) Hybrid (ResNet-50 [22])	0.5	62.50	74.20	67.80
2) Hybrid (DenseNet-201 [23])	0.3	64.37	87.50	74.17
2) Hybrid (DenseNet-201 [23])	0.5	55.75	75.78	64.24
2) Hybrid (InceptionV3 [24])	0.3	**78.99**	85.16	**81.95**
2) Hybrid (InceptionV3 [24])	0.5	**68.12**	73.44	70.68
3) End-to-end (YOLOv2 [26])	0.3	73.08	**89.06**	80.28
3) End-to-end (YOLOv2 [26])	0.5	67.31	**82.03**	**73.94**
3) End-to-end (Faster R-CNN [25])	0.3	66.90	74.22	70.37
3) End-to-end (Faster R-CNN [25])	0.5	45.07	50	47.41

P = precision, R = recall, F1 = F1-score

Quantitative results

Method	IoU	P	R	F1
1) Hand-crafted (SVM [29])	0.3	45.41	65.63	53.67
1) Hand-crafted (SVM [29])	0.5	41.62	60.16	49.20
2) Hybrid (ResNet-50 [22])	0.3	72.37	85.94	78.57
2) Hybrid (ResNet-50 [22])	0.5	62.50	74.20	67.80
2) Hybrid (DenseNet-201 [23])	0.3	64.37	87.50	74.17
2) Hybrid (DenseNet-201 [23])	0.5	55.75	75.78	64.24
2) Hybrid (InceptionV3 [24])	0.3	**78.99**	85.16	**81.95**
2) Hybrid (InceptionV3 [24])	0.5	**68.12**	73.44	70.68
3) End-to-end (YOLOv2 [26])	0.3	73.08	**89.06**	80.28
3) End-to-end (YOLOv2 [26])	0.5	67.31	**82.03**	**73.94**
3) End-to-end (Faster R-CNN [25])	0.3	66.90	74.22	70.37
3) End-to-end (Faster R-CNN [25])	0.5	45.07	50	47.41

P = precision, R = recall, F1 = F1-score

Quantitative results

Method	IoU	P	R	F1
1) Hand-crafted (SVM [29])	0.3	45.41	65.63	53.67
1) Hand-crafted (SVM [29])	0.5	41.62	60.16	49.20
2) Hybrid (ResNet-50 [22])	0.3	72.37	85.94	78.57
2) Hybrid (ResNet-50 [22])	0.5	62.50	74.20	67.80
2) Hybrid (DenseNet-201 [23])	0.3	64.37	87.50	74.17
2) Hybrid (DenseNet-201 [23])	0.5	55.75	75.78	64.24
2) Hybrid (InceptionV3 [24])	0.3	**78.99**	85.16	**81.95**
2) Hybrid (InceptionV3 [24])	0.5	**68.12**	73.44	70.68
3) End-to-end (YOLOv2 [26])	0.3	73.08	**89.06**	80.28
3) End-to-end (YOLOv2 [26])	0.5	67.31	**82.03**	**73.94**
3) End-to-end (Faster R-CNN [25])	0.3	66.90	74.22	70.37
3) End-to-end (Faster R-CNN [25])	0.5	45.07	50	47.41

P = precision, R = recall, F1 = F1-score

Discussion

- Three machine learning-based approaches:
  - Hand-crafted features
  - Hybrid
  - End-to-end
- ROI extractor
- Tiling strategy (scale limitations)
- Dataset of 358 annotated echograms
- Hybrid approach (IoU threshold 0.3)
- End-to-end approach (IoU threshold 0.5)

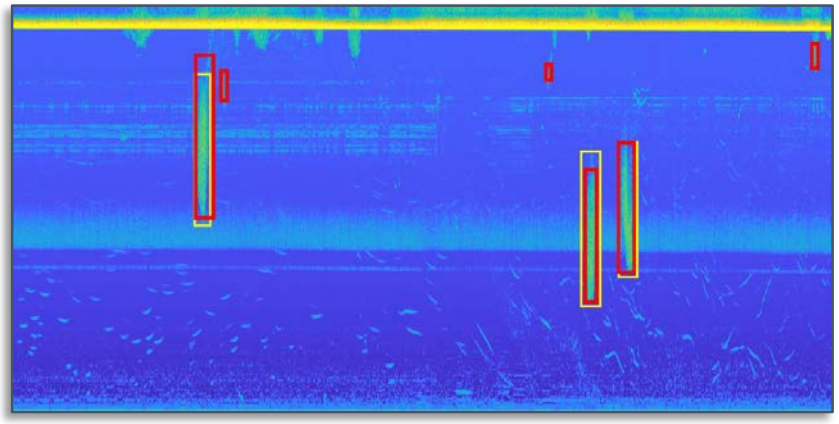

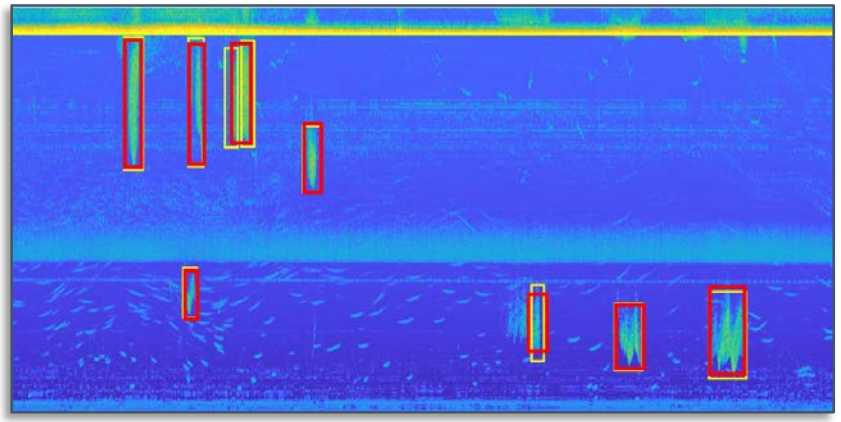

Discussion

- Three machine learning-based approaches:
  - Hand-crafted features
  - Hybrid
  - End-to-end
- ROI extractor
- Tiling strategy (scale limitations)
- Dataset of 358 annotated echograms
- Hybrid approach (IoU threshold 0.3)
- **End-to-end approach** (IoU threshold 0.5)

Scalable

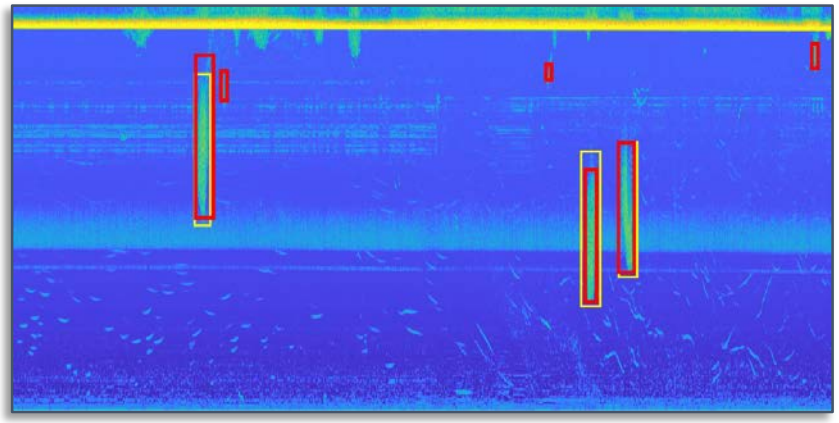

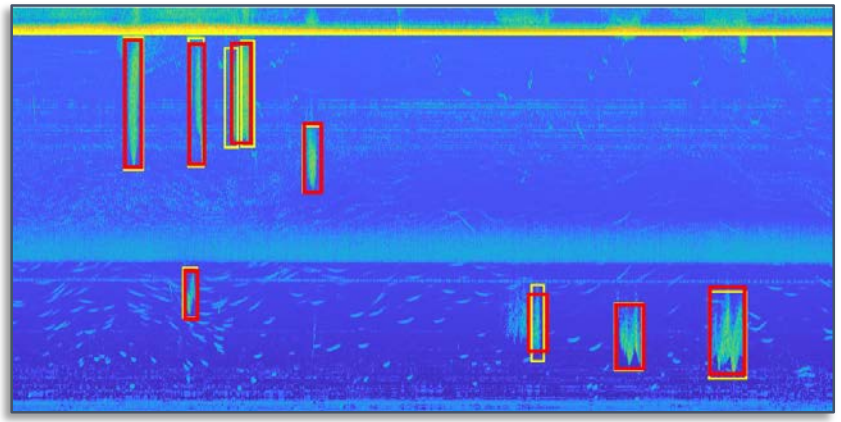

Thank you!

References

[1] D. Lemon, P. Johnston, J. Buermans, E. Loos, G. Borstad, and L. Brown, "Multiple-frequency moored sonar for continuous observations of zooplankton and fish," in *2012 Oceans*. IEEE, 2012, pp. 1–6.

[2] D. G. Reid, "Report on echo trace classification," *ICES Cooperative Research Report*, no. 238, 2000.

[3] T. K. Stanton, "30 years of advances in active bioacoustics: A personal perspective," *Method. Oceanogr.*, vol. 1-2, pp. 49–77, 2012.

[4] J. K. Horne, "Acoustic approaches to remote species identification: A review," *Fish. Oceanogr.*, vol. 9, no. 4, pp. 356–71, 2000.

[5] D. Reid, C. Scalabrin, P. Petitgas, J. Masse, R. Aukland, P. Carrera *et al.*, "Standard protocols for the analysis of school based data from echo sounder surveys," *Fish. Res.*, vol. 47, no. 2-3, pp. 125–36, 2000.

[6] P. LeFeuvre, G. Rose, R. Gosine, R. Hale, W. Pearson, and R. Khan, "Acoustic species identification in the Northwest Atlantic using digital image processing," *Fish. Res.*, vol. 47, no. 2-3, pp. 137–47, 2000.

[7] A. Charef, S. Ohshimo, I. Aoki, and N. Al Absi, "Classification of fish schools based on evaluation of acoustic descriptor characteristics," *Fish. Sci.*, vol. 76, no. 1, pp. 1–11, 2010.

[8] A. G. Cabreira, M. Tripode, and A. Madirolas, "Artificial neural networks for fish-species identification," *ICES J. Mar. Sci.*, vol. 66, no. 6, pp. 1119–29, 2009.

[9] H. Robotham, P. Bosch, J. C. Gutiérrez-Estrada, J. Castillo, and I. Pulido-Calvo, "Acoustic identification of small pelagic fish species in Chile using support vector machines and neural networks," *Fish. Res.*, vol. 102, no. 1-2, pp. 115–22, 2010.

[10] S. Gauthier, J. Oeffner, and R. L. O'Driscoll, "Species composition and acoustic signatures of mesopelagic organisms in a subtropical convergence zone, the New Zealand Chatham Rise," *Mar. Ecol. Prog. Ser.*, vol. 503, pp. 23–40, 2014.

[11] N. G. Fallon, S. Fielding, and P. G. Fernandes, "Classification of Southern Ocean krill and icefish echoes using random forests," *ICES J. Mar. Sci.*, vol. 73, no. 8, pp. 1998–2008, 2016.

[12] K. Malde, N. O. Handegard, L. Eikvil, and A.-B. Salberg, "Machine intelligence and the data-driven future of marine science," *ICES J. Mar. Sci.*, p. fsz057, 2019.

[13] Y. Hirama, S. Yokoyama, T. Yamashita, H. Kawamura, K. Suzuki, and M. Wada, "Discriminating fish species by an Echo sounder in a set-net using a CNN," in *21st Asia Pac. Symp. Intell. Evol. Syst. (IES)*. IEEE, 2017, pp. 112–5.

[14] Y. Shang and J. Li, "Study on echo features and classification methods of fish species," in *10th Int. Conf. Wirel. Commun. Signal Process. (WCSP)*. IEEE, 2018, pp. 1–6.

[15] O. Brautaset, A. U. Waldeland, E. Johnsen, K. Malde, L. Eikvil, A.-B. Salberg *et al.*, "Acoustic classification in multifrequency echosounder data using deep convolutional neural networks," *ICES J. Mar. Sci.*, 2020.

[16] R. J. Korneliussen, Y. Heggelund, G. J. Macaulay, D. Patel, E. Johnsen, and I. K. Eliassen, "Acoustic identification of marine species using a feature library," *Method. Oceanogr.*, vol. 17, pp. 187–205, 2016.

[17] L. Liu, H. Lu, Z. Cao, and Y. Xiao, "Counting fish in sonar images," in *25th IEEE Int. Conf. Image Process. (ICIP)*. IEEE, 2018, pp. 3189–93.

[18] D. Glukhov, R. Bohush, J. Mäkiö, and T. Hlukhava, "A joint application of fuzzy logic approximation and a deep learning neural network to build fish concentration maps based on sonar data," in *2nd Int. Workshop Comput. Model. Intell. Syst. (CMIS)*, 2019, pp. 133–42.

[19] G. French, M. Mackiewicz, M. Fisher, M. Challiss, P. Knight, B. Robinson *et al.*, "JellyMonitor: automated detection of jellyfish in sonar images using neural networks," in *14th IEEE Int. Conf. Signal Process. (ICSP)*. IEEE, 2018, pp. 406–12.

References

[20] H. Wang, Y. Yu, Y. Cai, X. Chen, L. Chen, and Q. Liu, "A comparative study of state-of-the-art deep learning algorithms for vehicle detection," *IEEE Intell. Transp. Syst. Mag.*, vol. 11, no. 2, pp. 82–95, 2019.

[21] S. H. Kassani and P. H. Kassani, "A comparative study of deep learning architectures on melanoma detection," *Tissue Cell*, vol. 58, pp. 76–83, 2019.

[22] K. He, X. Zhang, S. Ren, and J. Sun, "Deep residual learning for image recognition," in *IEEE Conf. Comput. Vis. Pattern Recognit. (CVPR)*, 2016, pp. 770–8.

[23] G. Huang, Z. Liu, L. Van Der Maaten, and K. Q. Weinberger, "Densely connected convolutional networks," in *IEEE Conf. Comput. Vis. Pattern Recognit. (CVPR)*, 2017, pp. 4700–8.

[24] C. Szegedy, V. Vanhoucke, S. Ioffe, J. Shlens, and Z. Wojna, "Rethinking the inception architecture for computer vision," in *IEEE Conf. Comput. Vis. Pattern Recognit. (CVPR)*, 2016, pp. 2818–26.

[25] S. Ren, K. He, R. Girshick, and J. Sun, "Faster R-CNN: Towards real-time object detection with region proposal networks," in *Adv. Neural Inf. Process. Syst. (NIPS)*, 2015, pp. 91–9.

[26] J. Redmon and A. Farhadi, "YOLO9000: better, faster, stronger," in *IEEE Conf. Comput. Vis. Pattern Recognit. (CVPR)*, 2017, pp. 7263–71.

[27] A. Rezvanifar, T. P. Marques, M. Cote, A. B. Albu, A. Slonimer, T. Tolhurst *et al.*, "A deep learning-based framework for the detection of schools of herring in echograms," *arXiv preprint arXiv:1910.08215*, 2019.

[28] D. Bradley and G. Roth, "Adaptive thresholding using the integral image," *J. Graph. Tools*, vol. 12, no. 2, pp. 13–21, 2007.

[29] C. Cortes and V. Vapnik, "Support-vector networks," *Mach. Learn.*, vol. 20, no. 3, pp. 273–97, 1995.

[30] R. Girshick, "Fast R-CNN," in *IEEE Conf. Comput. Vis. Pattern Recognit. (CVPR)*, 2015, pp. 1440–8.

[31] D. P. Kingma and J. Ba, "Adam: A method for stochastic optimization," *arXiv preprint arXiv:1412.6980*, 2014.

[32] J. Kiefer and J. Wolfowitz, "Stochastic estimation of the maximum of a regression function," *Ann. Math. Statist.*, vol. 23, no. 3, pp. 462–6, 1952.